Shielding and Activation Analyses for Outboard Region of FESS-FNSF Design

M.T. Elias and L. El-Guebaly

Fusion technology institute
University of Wisconsin – Madison
1500 Engineering drive
Madison, WI 53706

http://fti.neep.wisc.edu/

November 2015

UWFDM-1424

Abstract

The design of the outboard region of the Fusion Nuclear Science facility has to take into account several parameters, some of which are concerned with the structural degradation of materials. The composition of components has to meet the required shielding for the LTS magnet to operate as well as being sustainable under the normal operation conditions. DPA, He and H productions, and nuclear heating are all parameters that influence the design and are evaluated in this report for the outboard region of FNSF. The environmental aspects are evaluated for the induced activation using the ALARA code for different waste management options. Other safety issues related to accidents are also discussed in this report.

I. Introduction

The U.S. has taken a different pathway towards reaching a sustainable commercial fusion power plant than Europe, Korea and Japan. The preference in the U.S. a two-machine pathway, the first being the Fusion Nuclear Science Facility (FNSF) followed by a DEMO, which presents power plant operations and generates electricity using the anticipated technologies for commercial power plants [1]. The approach that is encouraged by Europe, Japan and korea is building a DEMO as a single step to a power plant but using two phases: Phase I would have the mission of filling the research gap needed for advancements in fusion; Phase II would be the rebuild of the facility to be a true DEMO. A third approach is the one based on a Pilot plant that uses power plant relevant technologies as much as practically possible and generates a small amount of electricity in a configuration scalable to a DEMO and Ultimately to a power plant.

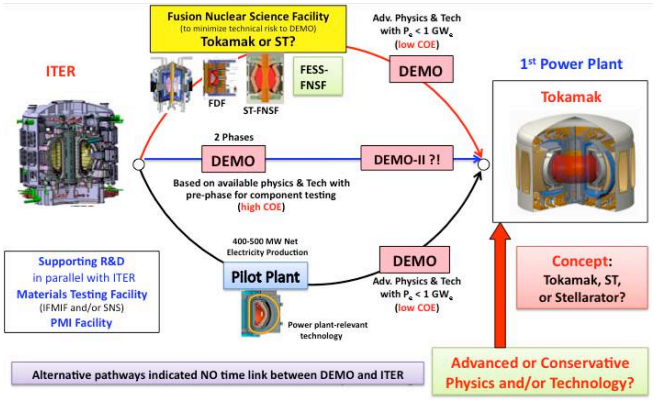

Figure 1:Potential pathways from ITER to first commercial power plant.

The main mission of the FNSF is to help resolve the scientific and technical issues in order to achieve fusion energy. ITER (International Thermonuclear Experimental Reactor) is set to resolve the issue of controlling high-performance burning plasmas, and taming the plasma material interface with very low fluence (~0.3 MWy/m^2). The purpose of the FNSF is to operate with long pulses in fully integrated systems to help overcome the technical challenges. If ITER is successful it will pave the way towards more advanced fusion devices [1].

The purpose of the first part of this study is to help design the outboard shielding components by choosing between different candidate materials that are used as fillers and validate the choice by providing values of the relevant nuclear parameters. The calculated parameters are the nuclear heating at the outboard (OB) mid plane, the radiation damage to the ferritic steel (FS) structure, including the displacement per atom (DPA), He and H production, and the distributions of the

gamma and neutron spectra in different regions. The analysis was performed on a simplified 1-D model using actual operating conditions of the FNSF design parameters listed in Table 1.

Table 1: FNSF operating parameters

Major Radius	4.8 m
Minor Radius	1.2 m
A	4
Fusion Power	526 MW
Peak OB NWL	1.8 MW/m^2
Plant Lifetime	~30 years ~8.5 FPY
Availability	~27% average

Concerning the environmental aspect, fusion devices have clear advantages when compared to fission devices, in that they only produce short-lived radioactive waste, which is highly preferred over the long term. Nevertheless, attention should be paid to decreasing the impact of activated materials. The activation of materials is due to the interactions between the constituents and neutrons generated from the plasma. The activation level depends directly on the radial distance between the constituent and plasma since the neutron flux decreases as one moves away from the source. The second part of this report examines the environmental aspects, such as the different rad-waste management scheme. An important safety issue, the decay heat, will be discussed as well.

II.Codes and Analysis

Four codes have been used in this study:

- DANTSYS (developed by Los Alamos National Laboratory) uses discrete ordinate neutral particle transport code [10] and FENDL-2 cross section data library [11] to calculate the neutron and gamma flux.
- Xspecs (Developed by University of Wisconsin) used to obtain the neutron and gamma flux spectra.
- Xmgrace (Developed by University of Wisconsin) used to plot the spectra produced by Xspecs.
- ALARA (Analytic and Laplacian Adaptive Radioactivity Analysis) (Developed by University of Wisconsin) [12] used to calculate the activation and related response functions using the FENDL-3 activation library [13] .

Different parameters were determined using the four codes. Shielding and activation analysis were performed to determine:

- ❖ Best candidate material to be used as a filler
- ❖ Optimization of the filler and coolant content
- ❖ Radial distribution of nuclear heating at OB mid plane
- ❖ Radial distribution of dpa, He and H production.
- ❖ Neutron and Gamma Flux spectra in various components
- ❖ Variation of specific activity with time after shutdown
- ❖ Classification of rad-waste
- ❖ Decay heat generated by components
- ❖ Clearance Index for all components
- ❖ Recycling Dose in Sv/h for all components.

III.Model, Radial Build and Methodology

A one-dimensional model was developed to mimic the original 3D design of the FNSF design shown in Fig.2. The composition of the outboard LT shield and the structural ring will be optimized based on this study. This analyses focuses on the outboard (OB) region of the model. The inboard region was added to the 1-D model to account for the backscattering of neutrons from it.

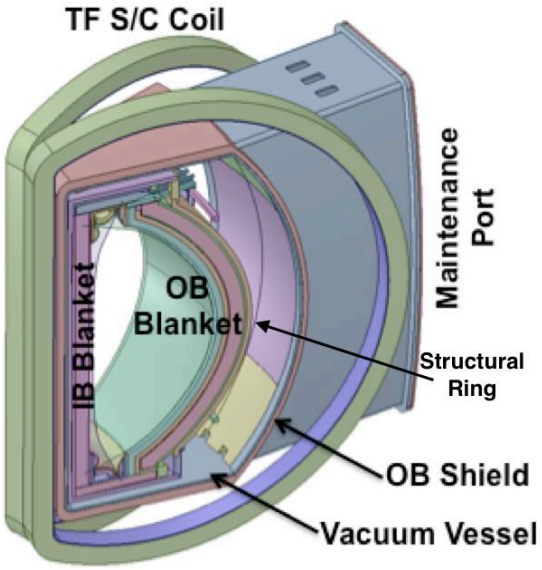

Figure 2:Fusion Energy System Study (FESS) –FNSF

Inboard region:
As the inboard (IB) region is not the main purpose of this study, a summary of the IB composition and radial build is given below, but details of its analysis are provided in reference [2]:

2 mm W armor	91.3% W, 8.7% void
3.8 cm FW	34% FS (MF82H) structure, 66% He
43 cm Breeding Zone	80% LiPb (90% Li-6), 12% He/void, 5% FS, 3% SiC
3 cm Back Wall	80% FS (MF82H) structure, 20% He
20 cm Structural Ring	28% FS (MF82H) structure, 20% He, 52% WC Filler
10 cm VV	43% MF82H structure, 51% WC Filler, 10% He
23 cm LT Shield	30% 3Cr-FS structure, 37 % WC Filler, 33% H_2O
23/7 cm Coil Case	100% SS-316LN
63 cm Winding Pack	30% JK2LB Steel, 25% Cu, 25% Ternary Nb_3Sn, 10% Hybrid Electric Insulator, 10% Liquid He

Figure 3 is a visual graph of the 1D radial build that was used as a model for the inboard region:

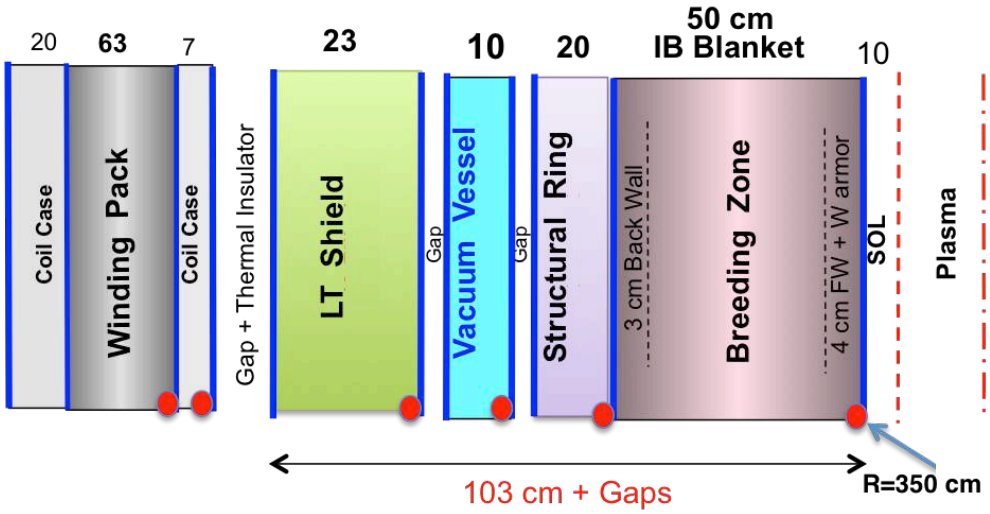

Figure 3: Inboard Radial Build

Outboard region:

For the purpose of simplifying the analysis the region of interest was assumed to have no penetrations or gaps between toroidal modules. The regions were homogenized for the activation analysis. Figure 4 is a visual graph of the 1D radial build that was used as a model for the outboard region.

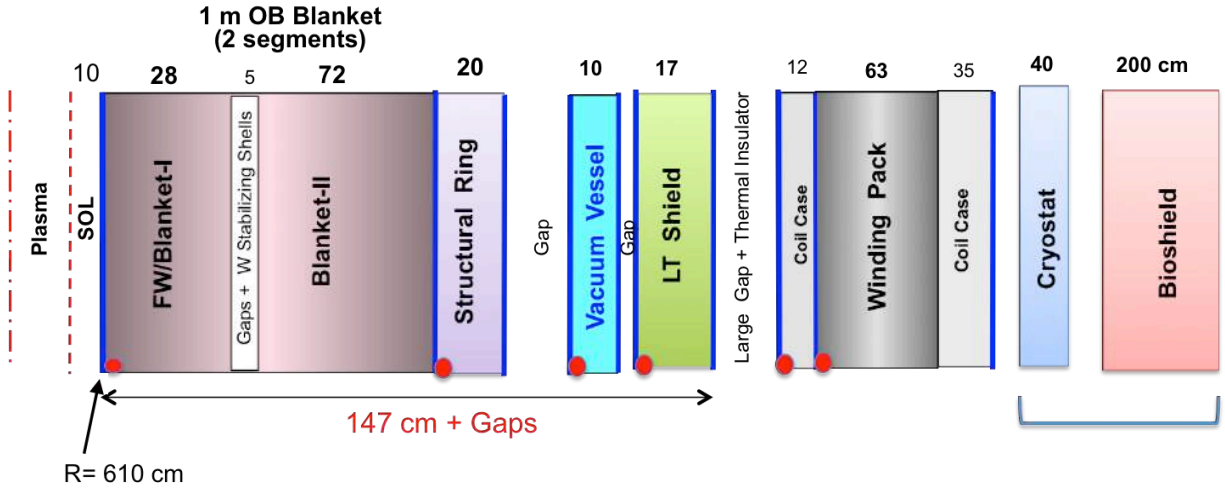

Figure 4: Outboard Region Radial build

Figure 5: SR and LT shield composition

The red dots in Figure 4 represent the locations where the analysis was performed for peak radiation damage at these components. The type of materials that would be used as filler in the structural ring (SR) and LT shield; are yet to be determined from shielding optimization analysis.

The cryostat and the bioshield are not included in the shielding analysis that was performed using DANTSYS, but they play a major role in the activation analysis. The compositions used for the shielding analysis are listed below with the red highlights referring to the yet to be determined composition:

2 mm W armor	91.3% W, 8.7% void
3.8 cm FW	34% FS (MF82H) structure, 66% He
21 cm Breeding Zone-I	73.7% LiPb 90,14.9% He/void,7.5% FS, 3.9% SiC
3 cm Back Wall for B-I	80% FS structure, 20% He
2 cm Stabilizing Shells	100% W alloy
3 cm Front Wall for B-II	80% FS (MF82H) structure, 20% He
66 cm Breeding Zone-II	73.7% LiPb90,14.9% He/void, 7.5% FS, 3.9% SiC
3 cm Back Wall for B-II	80% FS (MF82H) structure, 20% He
20 cm Structural Ring	5%FS (MF82H) structure, 20% He,75% ?? Filler
10 cm VV	60% 3Cr-FS structure, 40% He
17 cm LT Shield	5% 3Cr-FS structure, ??% ?? Filler, ??% H_2O
12 cm Coil Case	100% SS-316LN
63 cm Winding Pack	30% JK2LB Steel, 25% Cu, 25% Ternary Nb_3Sn, 10% Hybrid Electric Insulator, 10% Liquid He

The two candidate materials to be used as filler in the SR and VV are:

- MF82H (Low activation ferritic steel)
- B-FS (Borated ferritic steel)

The candidate materials are to be examined based on their effect on different important nuclear parameters at the OB magnet. These parameters include:

- Peak fast neutron fluence at Nb_3Sn superconductor
- Peak nuclear heating at WP (winding pack)
- Peak nuclear heating at coil case
- Peak dose at electric insulator
- Peak dpa at Cu stabilizer.

After the best filler option has been determined, shielding optimization analysis was performed to find the optimum composition for the LT shield that best meets the radiation limits for the magnet. These limits are listed in Table 2. Note that a higher dpa limit to the Cu stabilizer (6E-3) was considered based on the ARIES-ACT design [3], as the proposed limit for FNSF design (1E-4) seems too low.

Table 2: Operation Limits for the Magnet

Response Function	Limit
Peak fast n fluence to Ternary Nb_3Sn	3×10^{18} n/cm^2
Peak nuclear heating @ WP	1 mW/cm^3
Peak nuclear heating @ coil case	2 mW/cm^3
Peak dose to electrical insulator	5×10^{10} rads
Peak dpa to Cu stabilizer	10^{-4} dpa

The next step after determining the optimum composition is to check the distribution of nuclear heating that will be produced in various regions of FNSF. For the purpose of the structural integrity of the MF82H FS, the effect of radiation damage (dpa, He, H) that directly impacts the

lifetime of the components will be tested as well. The first part of the analysis is concluded with the flux distribution in different regions as we move outwards radially. The later part was calculated using Xspecs code and plots were generated using Xmgrace, both of which are codes developed by UW-Madison.

The second part of the analysis deals with the activation of solid materials, and their effects after shutdown on the environment. The cryostat and the bioshield were included in the analysis, as well as all impurities in the different constituents, which don't play a major role in neutron transport but are an important factor in the environmental aspects. DANTSYS code [10] was run to produce the neutron flux, which was then used by the ALARA code [12] to calculate the different parameters of activation.

The pathways from the plasma to the cryostat split into two, as the OB legs of the magnets don't completely cover the entire device. These two pathways are illustrated in Figure 6. Activation analysis was performed for both pathways separately.

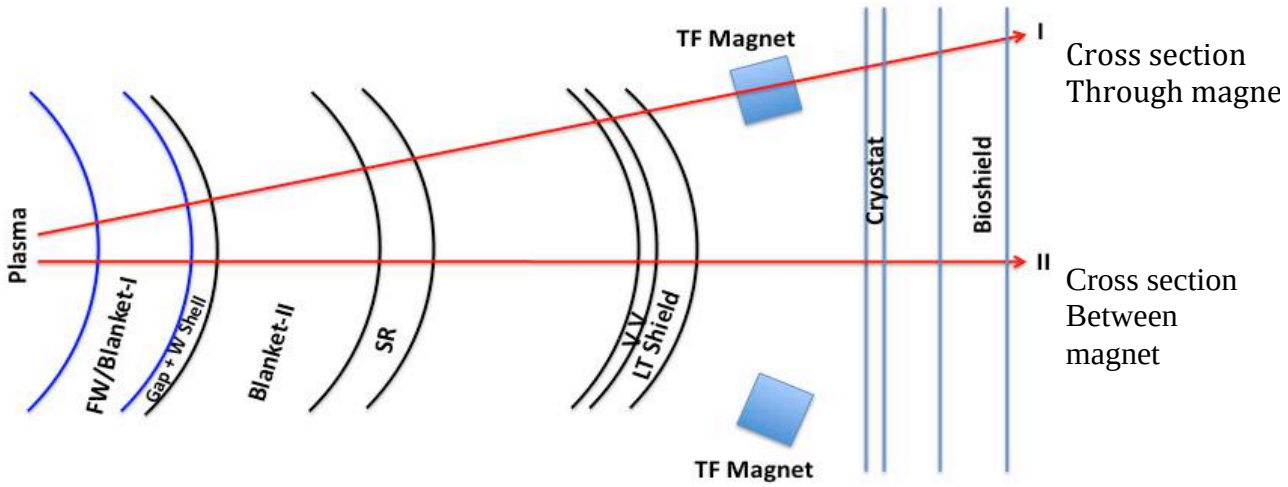

Figure 6: Pathways to the cryostat

The radiation-testing program that was proposed for the FESS-FNSF program consists of seven phases. Table 3 illustrates the seven phases of operation with their time frames, neutron exposure, plasma on/off times, and duty cycle [1].

Table 3: FESS-FNSF Program [1]

Fuel Cycle	He/H	D-D	D-T	D-T	D-T	D-T	D-T
	Plasma physics		Low Fluence Fusion Nuclear Break-in		High Fluence Fusion Nuclear Operation		
Phase	1	2	3	4	5	6	7
Phase Time (y)	1.5	2	3	5	5	7	7
FNSF Operating Time (y)	1.5	3.5	6.5	11.5	16.5	23.5	30.5
N_{n}^{peak}, MW/m^2		~0.009	1.5	1.5	1.5	1.5	1.5
Plasma on-time per year (days)	10-25% (37-91)	10-50% (37-183)	10-15% (37-55)	25% (91)	35% (128)	35% (128)	35% (128)
FPY			0.3 – 0.45	1.25	1.75	2.45	2.45
Peak EOL Fluence (MWy/m^2)			0.45-0.68	1.88	2.63	3.68	3.68
Cumulative EOL Fluence			0.68	2.56	5.19	8.87	12.55
Plasma duty cycle (days on/days off)		0.33-0.95 1/2 – 10/0.5	0.33 1/2	0.67 2/1	0.91 5/0.5	0.95 10/0.5	0.95 10/0.5
Operation / Maintenance per year (days)			111-165/254-200	137 / 228	141 / 224	135 / 230	135/230
Peak dpa			4.5-6.8	18.8	26.3	36.8	36.8
Cumulative dpa			6.8	25.6	51.9	88.7	125.5
Total # of plasma cycles			111-165	230	130	91	91

The lifetime expectancy differs between different components of the reactor. For the current planning purposes it is assumed that FW/blanket components will be capable of sustaining ~20dpa/200appm helium [1]. Different irradiation schedules are used for the various components with different lifetimes. These irradiation schedules are summarized in Table 4 and the different phases of operation are presented in Figure 7.

Table 4: Irradiation Schedules for various components

Group	Components	Irradiation Schedule
1	W-armor, FW/Blanket, W-shell	3 years with 15% availability (0.45 FPY) in Phase 3 + 5 years with 25% availability (1.25 FPY) in Phase 4
2	Structural Ring	3 years with 15% availability (0.45 FPY) in Phase 3 + 5 years with 25% availability (1.25 FPY) in Phase 4 + 5 years with 35% availability (1.75 FPY) in Phase 5
3	VV,LT Shield , Magnet , Cryostat, and Bioshield	3 years with 15% availability (0.45 FPY) in Phase 3 + 5 years with 25% availability (1.25 FPY) in Phase 4 + 19 years with 35% availability (6.65 FPY) in Phases 5,6,7

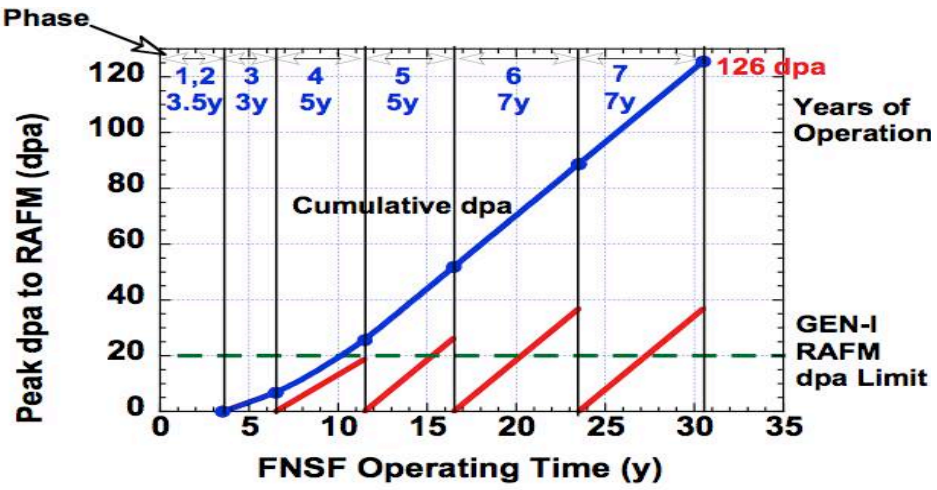

Figure 7: Irradiation damage and lifetime of RAFM structure at OB midplane of FNSF [1]

The parameters that were calculated using the ALARA code [12] in the second part of the study are listed below:

- Specific activity
- Waste disposal rating (WDR)
    - Fetter-Lo
    - Fetter-Hi
    - NRC-A
    - NRC-C
- Decay heat
- Recycling dose to equipment
- Clearance index
- Main contributors to above parameters.

IV.Shielding Results

The analysis results are discussed, explained and divided by the topics, starting with determining best material to be used as filler, choosing between two proposed candidates MF82H and B-FS. The following graphs show the comparisons that were made between the two fillers. The first comparison examined the peak fast neutron fluence (E_n>0.1 MeV) @8.5 FPY at Nb_3Sn. As Figure 8 shows, the B-FS candidate produces a lower fluence by a factor of ~1.6 making it a better candidate in terms of fluence.

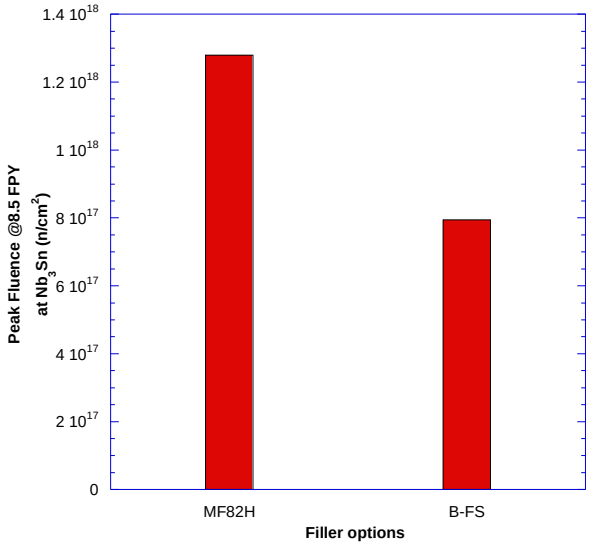

Figure 8: Peak fast neutron fluence @8.5 FPY at Nb_3Sn

Following the same steps, Figures 9-12 show that the B-FS results in lower damage compared to the MF82H by a factor of ~4 for the dose at insulator, peak nuclear heating at coil case and at the WP and a factor of ~1.5 for the peak dpa at Cu stabilizer

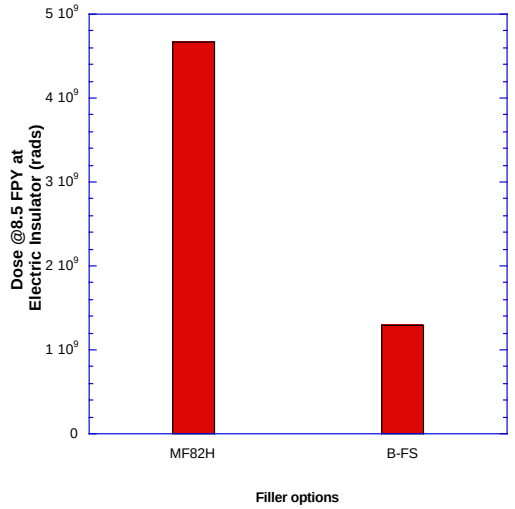

Figure 9: Dose to electric insulator

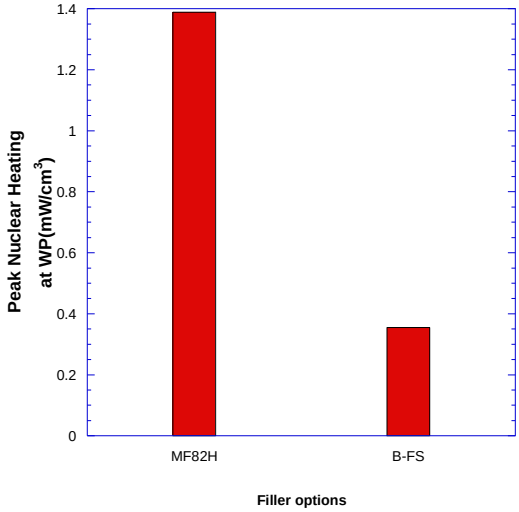

Figure 10: Peak nuclear heating at WP

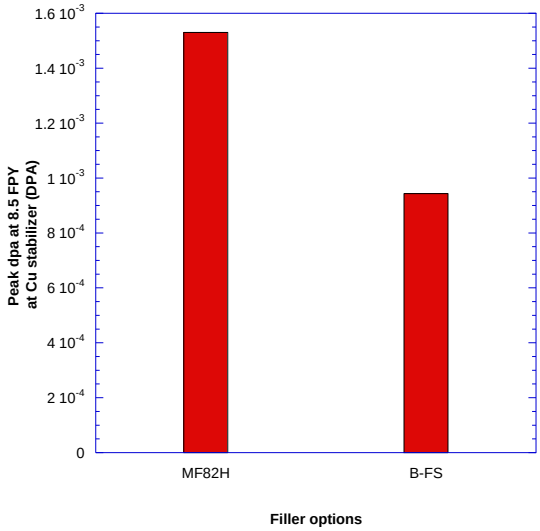

Figure 11:Peak dpa at Cu stabilizer

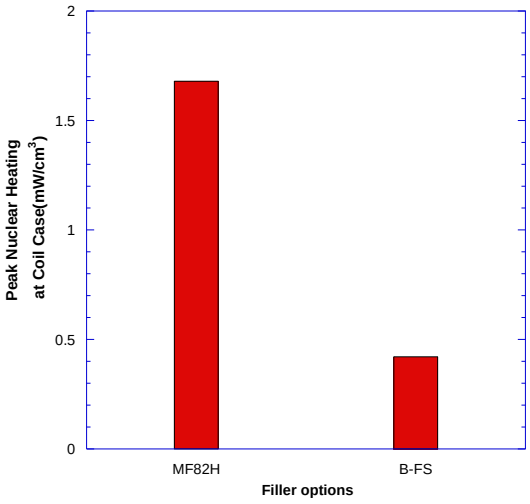

Figure 12:Peak nuclear heating at coil case

The results shown above prove that the B-FS is much better filler than MF82H, for all five of the radiation damage parameters examined for the magnet.

After deciding upon the filler material, the composition of the LT shield plays an important role in determining the magnet radiation level as well. The optimum filler and water contents will be determined. Figures 13 and 14 show that the percentage of filler used is highly determined by the heating at the coil case. All the values achieved at a composition of 50% H2O, 45%B-FS, 5% MF82H FS ribs meet the magnet radiation limits, except the heating at the coil case which is ~10% above the limit. An extra 1 cm of LT shield could be added to the design in order to meet the limit of nuclear heating at the coil case

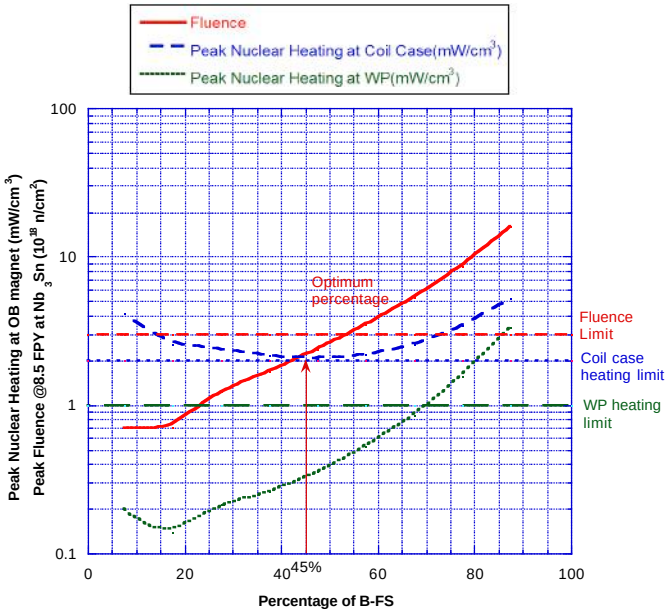

Figure 13: Effect of B-FS content in LT shield on magnet fluence and nuclear heating

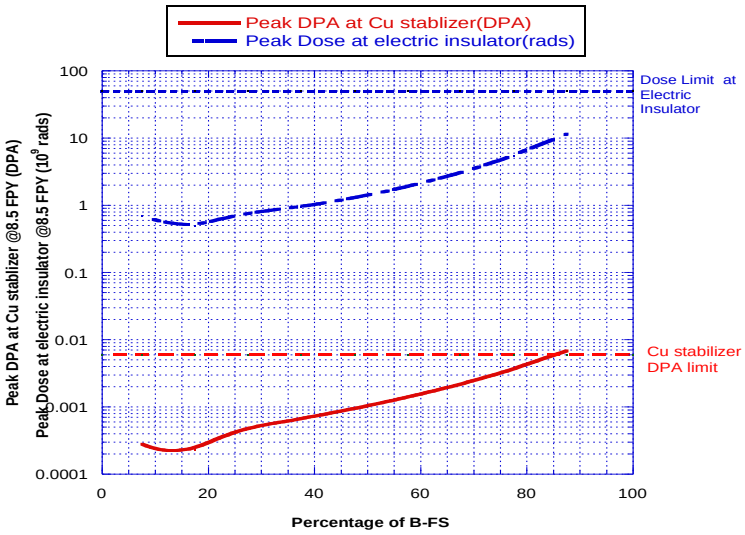

Figure 14: Effect of B-FS content in LT shield on dpa to Cu stabilizer and dose to insulator

The radial distribution of nuclear heating was calculated in each component of the radial build and plotted in Figure 15; the regions are named at the top of the graph. Some of the conclusions from the results are that the FS walls always produces less heating compared to the middle of SR and LT shield, as both contain B-FS filler and the LT shield contains water coolant. Less heating occurs in the VV, even though the VV was subjected to a higher energy neutron flux because the VV contain 40% of the coolant. The heating in regions after the breeding zone was multiplied by a factor of 3 to account for peak values due to the neutron streaming through the assembly gaps.

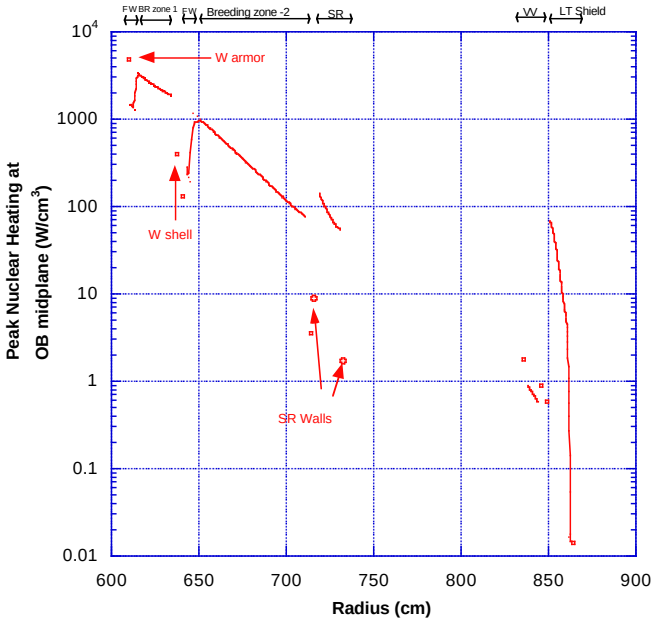

Figure 15: Nuclear heating at OB midplane

The radiation damage to structural material of the design (MF82H) was examined. The neutron flux was computed for the actual composition and then used to calculate radiation effect on MF82H instead of the actual material composition. The red squares on the graphs in Figures 16,17,18 are the points where the radiation damage was calculated for MF82H structure at the red dots in Figure 4. It can be see that the results perfectly match. It should also be noted that the

gradient for He and H is larger than that for dpa, because the He and H productions have a threshold energies below which damage does not occur. Table 5 presents the values at different regions and the ratio between them; the He/DPA ratio dramatically decreases.

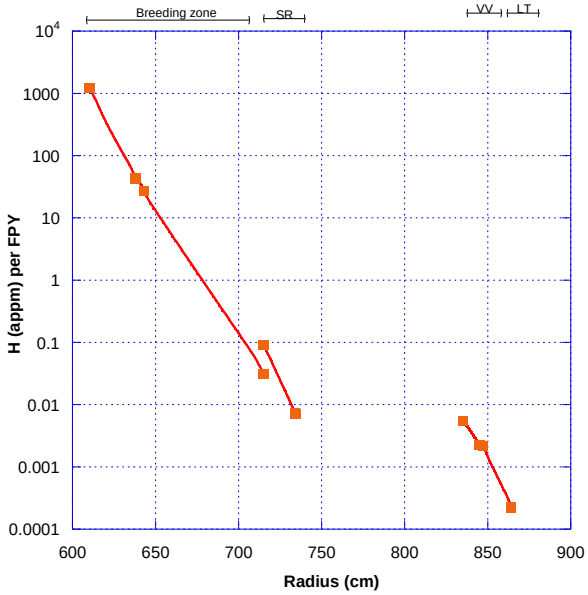

Figure 16: Hydrogen production in MF82H of OB components

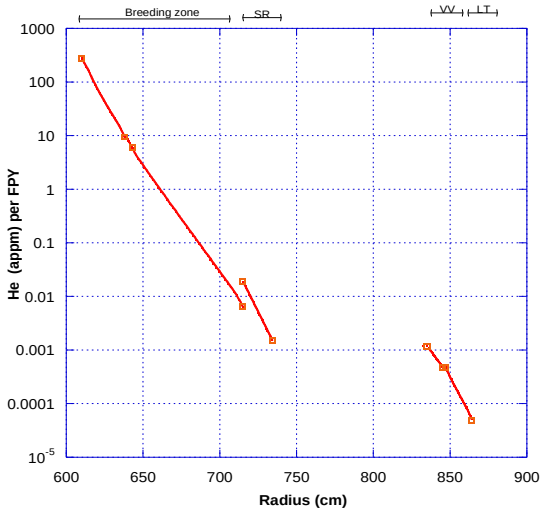

Figure 17: Helium production in MF82H of OB components

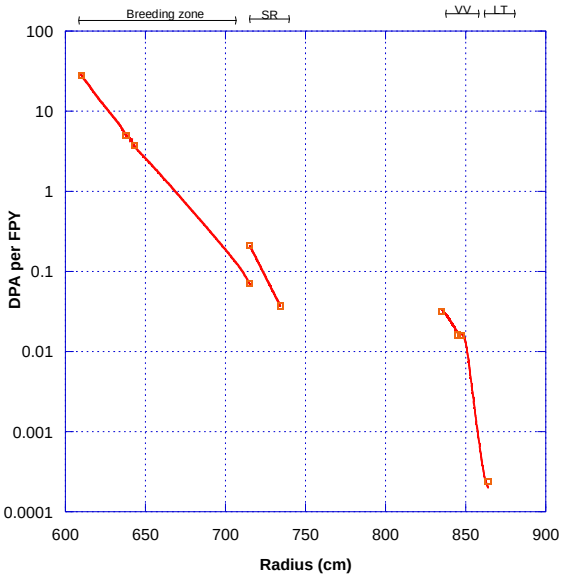

Figure 18: dpa per FPY in MF82H of OB components

Table 5: Radiation damage at different OB components

	dpa/FPY	He/FPY	H/FPY	He/dpa Ratio
FW	2.77E+01	2.72E+02	1.21E+03	9.84E+00
BW	4.95E+00	9.38E+00	4.30E+01	1.90E+00
FW2	3.75E+00	5.92E+00	2.71E+01	1.58E+00
BW2	7.04E-02	6.40E-03	3.07E-02	9.10E-02
SR	2.09E-01	1.89E-02	9.07E-02	9.05E-02
VV front	3.19E-02	1.15E-03	5.42E-03	3.62E-02
VV back	1.62E-02	4.78E-04	2.24E-03	2.95E-02
LT Front	1.59E-02	4.69E-04	2.20E-03	2.94E-02
LT Back	2.41E-04	4.91E-05	2.23E-04	2.04E-01

As the neutrons pass through the components, attenuation starts to decrease their energy and soften their flux. Absorption of neutrons also takes place, which causes the activation of the material. Gamma rays that are produced also experience absorption. They decrease in flux but do not get shifted to lower energies as for neutrons. This can be seen in Figures 19 and 20.

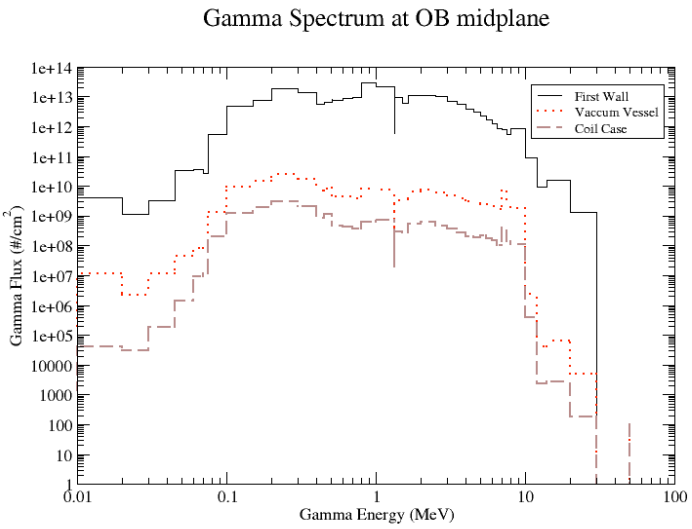

Figure 19:Gamma spectrum at various OB components

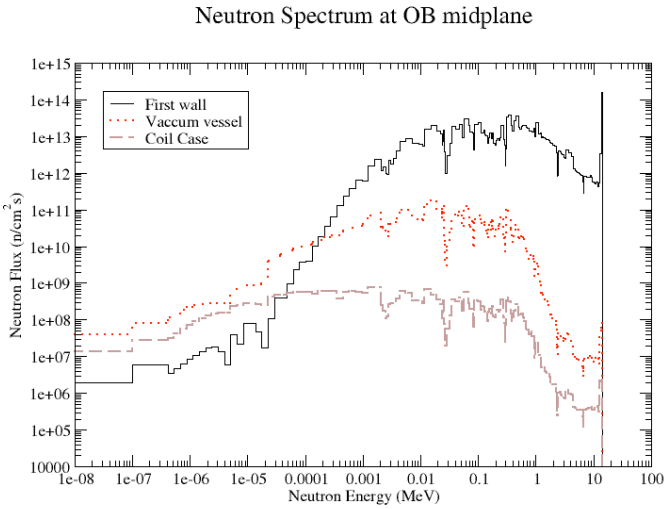

Figure 20: Neutron spectrum at various OB components

V.Activation Results

So far, our discussion has only been limited to the parameters during the time of operation. The environmental aspect becomes an important factor after shutdown. The specific activity of a material is the activity per meter cube of fully compressed material (doesn't contain voids). As the two pathways discussed previously produce different activation results, the two methods of analysis that were performed are typically composed of the same steps but yield different results specifically for the cryostat and bioshield.

V.A. Specific Activity

Using the ALARA code [12] and its data libraries, the specific activity was calculated for the different OB components of FNSF. As shown in Figures 21-24, the specific activity gradually decreases with time after shutdown. Components containing tungsten (W) have higher specific activity. This can also be noticed in Table 6, as tungsten is also the main contributor for the specific activity at shutdown. The contribution to the specific activity by tungsten at shutdown creates a significant increase but fades out at ~ 1 year. MF82H Contributors have longer half-lives and become the main contributors as seen in Table 7. This can be seen in Figures 21 and 22 where

W armor and W shell, which are rich in tungsten, exhibit greater activities by a factor of 5-20 at shutdown.

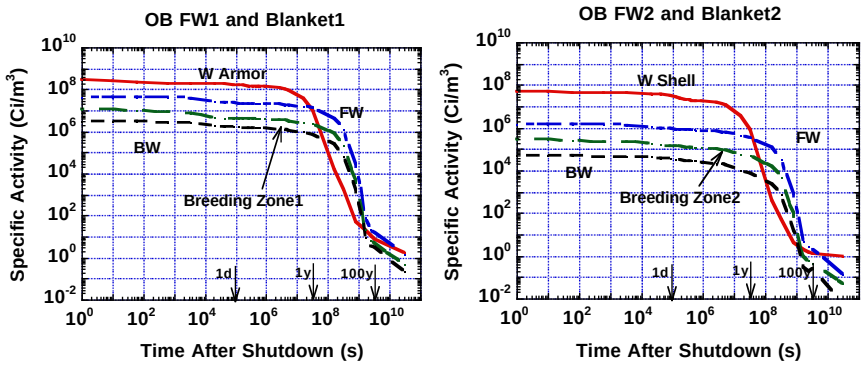

Figure 21:Specific Activity in FW/Blanket

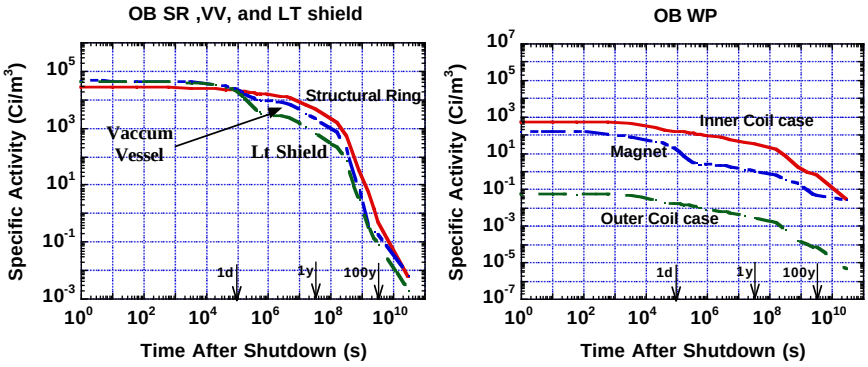

Figure 22: Specific Activity in SR, VV, LT shield, and magnet

The path taken by neutrons through the magnets produces lower specific activity values at the cryostat and bioshield than the one taken between the magnets, as the magnet provides additional shielding. The bioshield was divided into four layers 50 cm thick each. At the last layer of the bioshield where neutrons reach their lowest flux, Mo-98 starts to become the main contributor. Having very long half-life (>10^9 years), the specific activity doesn't decrease with time. This can be observed in Figure 23 and in Tables 6 and 7 where the main contributor is still Mo-98 at one year and beyond.

We checked the FENDL activation library and found out that the latest FENDL-3.0 library reclassified the very long-lived nuclides (what used to be classifies as "stable" in the Chart of Nuclides and Isotopes) as being radioactive with extremely long half-lives (> e12 years). Figure 24 displays the breakdown of Bioshield-4 activity for very long-lived nuclides (Ca-48, Ni-58, Mo-92, Mo-98, Mo-100 - marked here as stable) and all other radionuclides. This problem has never been observed in previous designs that used the FENDL-2 activation library. It is becoming more pronounced for regions with extremely low neutron flux, such as the outermost layer of the bioshield, where the activity of the radionuclides of interest are lower than that of the "background" activity caused by the decay of the very long lived nuclides. As will be shown later, the decay heat of Bioshield-4 exhibits the same behavior as the activity and the decay heat of the very long-lived nuclides, especially Mo-98, exceeds that of all other radionuclides.

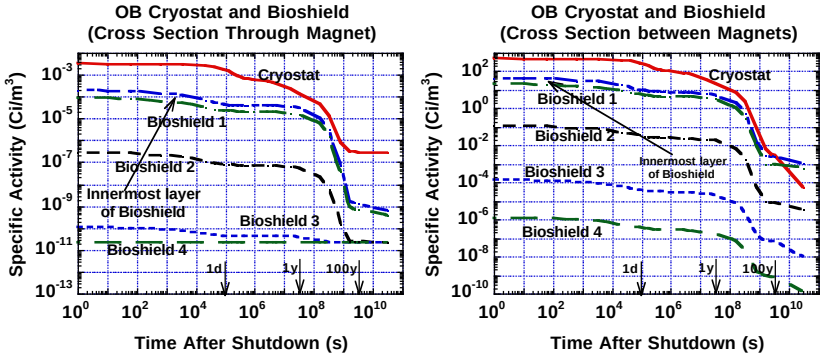

Figure 23:Specific activity for cryostat and bioshield.

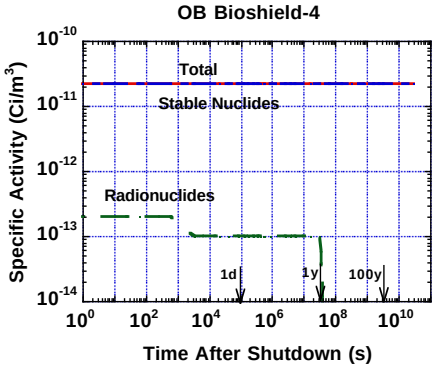

Figure 24: Breakdown of Bioshield-4 activity.

Table 6: Specific Activity of OB components at shutdown

Zones	Shutdown	Contributor			Contributions%		
W armor	2.90E+08	w-185	w-183m	w-181	32.14%	18.37%	17.03%
FW1	4.56E+07	mn-56	fe-55	cr-51	44.70%	33.83%	8.98%
BZ1	1.17E+07	mn-56	al-28	fe-55	31.12%	25.24%	23.16%
BW1	3.13E+06	mn-56	fe-55	cr-51	35.43%	28.31%	8.28%
W shell	5.16E+07	w-187	w-185	w-183m	47.17%	34.72%	11.70%
FW2	1.60E+06	mn-56	fe-55	w-187	29.22%	26.79%	12.07%
BZ2	2.95E+05	fe-55	w-187	mn-56	19.45%	15.52%	13.41%
BW2	5.20E+04	w-187	w-185	fe-55	31.58%	22.58%	16.27%
Structural ring	2.87E+04	w-187	w-185		29.24%	24.47%	
Vacuum vessel	4.56E+04	w-187	w-185	mn-56	57.51%	13.44%	12.02%
Out board shield	4.36E+04	w-187	w-183m	mn-56	77.69%	8.74%	5.42%
Inner coil case	5.02E+02	mn-56	cr-51	mo-99	53.99%	8.59%	7.77%
Winding pack	1.58E+02	nb-94m	cu-64	mn-56	42.76%	31.15%	16.04%
Outer coil case	5.66E-02	mn-56	mo-99	tc-99m	54.03%	9.14%	8.05%
Cryostat	3.42E-03	w-187	w-183m	w-185	69.55%	9.40%	6.88%
Front layer of bioshield	1.90E-04	mn-56	al-28	fe-55	34.50%	23.01%	19.90%
Bioshield1	8.64E-05	mn-56	al-28	fe-55	35.34%	27.04%	23.65%
Bioshield2	2.83E-07	mn-56	al-28	fe-55	35.22%	28.90%	25.34%
Bioshield3	1.07E-10	mn-56	al-28	mo-98	27.79%	23.52%	20.07%
Bioshield4	2.17E-11	mo-98	mn-56		98.75%	0.33%	

Between Magnets							
Cryostat	5.27E+02	w-187	w-183m	w-185	67.71%	9.31%	7.34%
Front layer of bioshield	4.59E+01	mn-56	al-28	fe-55	25.50%	17.63%	15.00%
Bioshield1	2.38E+01	mn-56	al-28	fe-55	25.28%	19.53%	16.96%
Bioshield2	1.32E-01	mn-56	al-28	fe-55	24.85%	20.52%	17.78%
Bioshield3	1.58E-04	mn-56	al-28	fe-55	24.16%	22.13%	16.88%
Bioshield4	1.45E-06	mn-56	al-28	fe-55	24.05%	22.19%	16.52%

Table 7:Specific Activity of OB components at 1 year after shutdown

Zones	1 year	Contributor			Contributions%		
W armor	9.61E+06	w-181	w-185	ta-182	63.89%	33.72%	1.00%
FW1	1.29E+07	fe-55	mn-54	w-181	92.79%	6.47%	0.30%
BZ1	2.30E+06	fe-55	mn-54	w-185	91.48%	7.60%	0.31%
BW1	7.64E+05	fe-55	mn-54	w-185	90.18%	8.20%	0.87%
W shell	7.93E+05	w-185	w-181	ta-179	78.45%	21.06%	0.25%
FW2	3.67E+05	fe-55	mn-54	w-185	90.44%	7.37%	1.32%
BZ2	4.88E+04	fe-55	mn-54	w-185	91.29%	5.28%	2.30%
BW2	7.20E+03	fe-55	w-185	ta-182	91.17%	5.66%	1.92%
Structural ring	4.59E+03	fe-55	w-185	ta-182	90.07%	5.31%	1.90%
Vacuum vessel	2.01E+03	fe-55	w-185	co-60	86.01%	10.61%	2.59%
Out board shield	6.43E+02	fe-55	w-185	co-60	83.22%	10.79%	4.28%
Inner coil case	3.01E+01	co-60	fe-55	ta-182	48.01%	42.25%	5.18%
Winding pack	1.07E+00	nb-93m	sb-125	fe-55	40.54%	21.97%	19.49%
Outer coil case	2.96E-03	co-60	fe-55	ta-182	46.91%	44.59%	4.34%
Cryostat	1.36E-04	fe-55	ta-182	w-185	80.13%	9.28%	5.99%
Front layer of bioshield	2.94E-05	fe-55	fe-59	s-35	99.95%	0.04%	0.01%
Bioshield1	1.59E-05	fe-55	fe-59	s-35	99.96%	0.03%	0.01%
Bioshield2	5.57E-08	fe-55	mo-98	fe-59	99.92%	0.04%	0.02%
Bioshield3	3.81E-11	mo-98	fe-55	ca-48	56.36%	43.39%	0.14%
Bioshield4	2.16E-11	mo-98	ca-48	fe-55	99.56%	0.25%	0.18%
Between Magnets							
Cryostat	2.38E+01	fe-55	ta-182	w-185	81.14%	8.45%	5.63%
Front layer of bioshield	5.43E+00	fe-55	ca-45	mn-54	98.28%	1.52%	0.07%
Bioshield1	3.19E+00	fe-55	ca-45	mn-54	98.44%	1.55%	0.03%
Bioshield2	1.85E-02	fe-55	ca-45	mn-54	98.04%	1.57%	0.08%
Bioshield3	2.13E-05	fe-55	ca-45	mn-54	97.25%	1.52%	0.79%
Bioshield4	1.92E-07	fe-55	ca-45	mn-54	96.90%	1.52%	1.00%

V.B. Waste Disposal Rating

The waste disposal rating (WDR) is the ratio between the specific activity and the allowable limit summed over all radioisotopes. The method of disposal differs for each class of waste. According to US Nuclear Regulatory Commission (NRC) 10CFR61 document [5] requirements are present for each class of rad waste. The NRC classifies Low Level Waste (LLW) into three classes A, B, and C, according to its specific activity level. Class A being the least hazardous waste and can be disposed of in containers placed at ~5 m deep in ground. Class C LLW is of specific interest because activation of fusion materials generates some long-lived radioisotopes. As the NRC ratings are only available for 8 radionuclides with z<55 besides actinides, in 1990 Fetter [6] determined the Class C LLW specific activity limits for all radionuclides of interest to fusion. The results displayed in Table 8 show that all material can be classified as Class A LLW except the FW. When changing the structural material from MF82H to MF82H_present [3] the values highlighted in red with an "*" are reduced to 2.48E-01, 1.47E-01 and 1.56E-01 respectively, meaning all OB components can be classified as Class A LLW with impurity control.

Table 8: WDR of OB components evaluated at 100y after shutdown

OB Zones	Fetter-Hi	Fetter-Lo	NRC-C	NRC-A
W armor	4.61E-02	1.38E-01	9.66E-03	1.05E-01
FW1	1.73E-01	2.30E-01	1.47E-01	1.84E+00*
BZ1	9.14E-02	1.12E-01	8.31E-02	9.36E-01
BW1	1.11E-01	1.31E-01	1.01E-01	1.09E+00*
W/FW/Blanket	1.14E-01	1.44E-01	1.01E-01	1.15E+00*
W shell	3.18E-03	2.59E-02	1.15E-02	1.16E-01
FW2	8.68E-02	1.01E-01	7.93E-02	8.42E-01
BZ2	2.11E-02	2.45E-02	1.97E-02	2.08E-01
BW2	7.07E-03	8.22E-03	6.54E-03	6.97E-02
W/FW/Blanket (2)	2.68E-02	3.41E-02	2.58E-02	2.73E-01
Structural ring	6.82E-03	7.97E-03	6.32E-03	6.77E-02
Vacuum vessel	7.32E-03	8.71E-03	6.53E-03	6.99E-02
Out board shield	2.08E-03	2.53E-03	1.70E-03	1.89E-02
Inner Coil case	3.30E-03	1.91E-02	1.75E-03	3.40E-02
Insulator 1	6.00E-07	5.85E-06	4.38E-05	4.38E-04
Winding pack	1.40E-01	1.40E-01	1.40E-01	1.40E+00
Insulator 2	2.45E-10	2.42E-09	1.81E-08	1.81E-07
Outer Coil case	4.51E-07	2.54E-06	2.38E-07	3.96E-06
Magnet average	7.57E-02	7.75E-02	7.56E-02	7.58E-01
Cryostat	5.38E-09	5.46E-09	3.00E-10	3.47E-09
Front layer of bioshield	5.58E-12	7.62E-12	1.42E-11	1.57E-10
Bioshield1	1.29E-12	2.15E-12	5.70E-12	6.53E-11
Bioshield2	2.30E-15	4.95E-15	1.75E-14	2.05E-13
Bioshield3	1.32E-18	2.19E-18	5.28E-18	6.20E-17
Bioshield4	9.73E-21	1.27E-20	1.37E-20	1.63E-19

Between Magnets				
Cryostat	6.16E-08	6.56E-08	6.51E-07	8.63E-05
Front layer of bioshield	1.77E-07	5.37E-07	1.89E-06	2.17E-05
Bioshield1	7.60E-08	2.64E-07	9.40E-07	1.11E-05
Bioshield2	5.79E-10	1.67E-09	5.24E-09	6.21E-08
Bioshield3	3.46E-12	5.09E-12	6.15E-12	7.46E-11
Bioshield4	4.13E-14	5.70E-14	5.65E-14	6.90E-13

The main contributor for most WDRs is Nb-94, as we could see in the Tables 9,10,11,12.

Table 9: WDR for Fetter-Hi limits evaluated at 100y after shutdown

Zones	Fetter Hi	Contributor			Contributions%		
W armor	4.61E-02	re-186m	tc-99	nb-94	47.30%	22.13%	17.77%
FW1	1.73E-01	nb-94	ho-166m	tc-99	83.09%	6.64%	3.64%
BZ1	9.14E-02	nb-94	ho-166m	tc-99	87.87%	7.09%	2.45%
BW1	1.11E-01	nb-94	ho-166m	tc-99	89.75%	7.14%	1.95%
W shell	3.18E-03	tc-99	re-186m	c-14	68.53%	14.93%	4.41%
FW2	8.68E-02	nb-94	ho-166m	tc-99	90.50%	7.17%	1.84%
BZ2	2.11E-02	nb-94	ho-166m	tc-99	90.92%	6.82%	1.75%
BW2	7.07E-03	nb-94	ho-166m	tc-99	91.99%	6.03%	1.81%
Structural ring	6.82E-03	nb-94	ho-166m	tc-99	92.03%	5.96%	1.86%
Vacuum vessel	7.32E-03	nb-94	ho-166m	tc-99	88.68%	8.98%	2.12%
Out board shield	2.08E-03	nb-94	ho-166m	tc-99	80.83%	16.50%	2.39%
Inner Coil case	3.30E-03	tc-99	nb-94	ni-59	53.09%	46.41%	0.36%
Insulator 1	6.00E-07	c-14	al-26	be-10	97.32%	2.72%	0.00%
Winding pack	1.40E-01	nb-94	tc-99	ag-108m	99.77%	0.01%	0.00%
Insulator 2	2.45E-10	c-14	al-26	be-10	98.49%	1.37%	0.00%
Outer Coil case	4.51E-07	tc-99	nb-94	ni-59	51.48%	48.15%	0.24%
Cryostat	5.38E-09	u-235	u-234	th-230	56.32%	27.32%	9.50%
Front layer of bioshield	5.58E-12	nb-94	k-40	c-14	91.22%	4.28%	2.15%
Bioshield1	1.29E-12	nb-94	k-40	c-14	81.92%	9.97%	4.71%
Bioshield2	2.30E-15	nb-94	k-40	c-14	64.41%	19.76%	9.14%
Bioshield3	1.32E-18	ar-39	nb-94	k-40	45.18%	35.93%	10.16%
Bioshield4	9.73E-21	ar-39	nb-94	k-40	74.44%	18.10%	3.22%
Between Magnets							
Cryostat	6.16E-08	ni-59	u-235	u-234	90.93%	4.92%	2.39%
Front layer of bioshield	1.77E-07	ar-39	k-40	ca-41	38.36%	24.53%	17.11%
Bioshield1	7.60E-08	k-40	ca-41	ar-39	33.54%	23.28%	19.20%
Bioshield2	5.79E-10	ar-39	k-40	ca-41	38.50%	25.55%	17.78%
Bioshield3	3.46E-12	ar-39	k-40	ca-41	86.95%	5.11%	3.32%
Bioshield4	4.13E-14	ar-39	k-40	ca-41	89.61%	3.95%	2.52%

Table 10: WDR for Fetter-Lo limits evaluated at 100y after shutdown

Zones	Fetter Lo	Contributor			Contributions%		
W armor	1.38E-01	tc-99	re-186m	nb-94	73.85%	15.78%	5.93%
FW1	2.30E-01	nb-94	tc-99	ho-166m	62.58%	27.38%	5.00%
BZ1	1.12E-01	nb-94	tc-99	ho-166m	71.83%	20.04%	5.80%
BW1	1.31E-01	nb-94	tc-99	ho-166m	76.34%	16.57%	6.08%
W shell	2.59E-02	tc-99	c-14	re-186m	90.11%	5.80%	1.96%
FW2	1.01E-01	nb-94	tc-99	ho-166m	77.64%	15.81%	6.15%
BZ2	2.45E-02	nb-94	tc-99	ho-166m	78.45%	15.08%	5.88%
BW2	8.22E-03	nb-94	tc-99	ho-166m	79.11%	15.58%	5.18%
Structural ring	7.97E-03	nb-94	tc-99	ho-166m	78.83%	15.94%	5.11%
Vacuum vessel	8.71E-03	nb-94	tc-99	ho-166m	74.48%	17.79%	7.54%
Out board shield	2.53E-03	nb-94	tc-99	ho-166m	66.51%	19.68%	13.58%
Inner Coil case	1.91E-02	tc-99	nb-94	ni-59	91.77%	8.02%	0.06%
Insulator 1	5.85E-06	c-14	al-26	be-10	99.76%	0.28%	0.00%
Winding pack	1.40E-01	nb-94	tc-99	ag-108m	99.72%	0.06%	0.00%
Insulator 2	2.42E-09	c-14	al-26	be-10	99.72%	0.14%	0.00%
Outer Coil case	2.54E-06	tc-99	nb-94	ni-59	91.25%	8.54%	0.04%
Cryostat	5.46E-09	u-235	u-234	th-230	55.51%	26.93%	9.36%
Front layer of bioshield	7.62E-12	nb-94	c-14	tc-99	66.75%	15.74%	8.68%
Bioshield1	2.15E-12	nb-94	c-14	cl-36	49.28%	28.31%	10.32%
Bioshield2	4.95E-15	c-14	nb-94	cl-36	42.40%	29.88%	15.89%
Bioshield3	2.19E-18	c-14	ar-39	nb-94	28.75%	27.16%	21.60%
Bioshield4	1.27E-20	ar-39	nb-94	c-14	57.20%	13.90%	12.32%
Between Magnets							
Cryostat	6.56E-08	ni-59	ni-63	u-235	85.33%	6.40%	4.62%
Front layer of bioshield	5.37E-07	c-14	ca-41	cl-36	46.37%	16.87%	15.75%
Bioshield1	2.64E-07	c-14	ca-41	cl-36	46.90%	20.12%	17.51%
Bioshield2	1.67E-09	c-14	ca-41	cl-36	41.28%	18.48%	17.52%
Bioshield3	5.09E-12	ar-39	c-14	cl-36	59.15%	15.84%	14.62%
Bioshield4	5.70E-14	ar-39	cl-36	c-14	64.96%	13.50%	12.99%

Table 11: WDR for NRC-C limits evaluated at 100y after shutdown

Zones	NRCC	Contributor			Contributions%		
W armor	9.66E-03	nb-94	c-14	tc-99	84.78%	12.53%	2.11%
FW1	1.47E-01	nb-94	ni-63	ni-59	97.91%	1.33%	0.88%
BZ1	8.31E-02	nb-94	c-14	ni-63	96.63%	2.03%	0.66%
BW1	1.01E-01	nb-94	ni-59	ni-63	98.64%	0.48%	0.39%
W shell	1.15E-02	c-14	tc-99	ni-59	99.52%	0.41%	0.04%
FW2	7.93E-02	nb-94	ni-59	ni-63	99.17%	0.46%	0.33%
BZ2	1.97E-02	nb-94	c-14	ni-59	97.64%	1.42%	0.42%

BW2	6.54E-03	nb-94	ni-63	ni-59	99.35%	0.34%	0.27%
Structural ring	6.32E-03	nb-94	ni-63	ni-59	99.40%	0.31%	0.25%
Vacuum vessel	6.53E-03	nb-94	ni-63	ni-59	99.31%	0.37%	0.23%
Out board shield	1.70E-03	nb-94	ni-63	ni-59	99.00%	0.60%	0.32%
Inner Coil case	1.75E-03	nb-94	ni-63	ni-59	87.53%	4.98%	2.79%
Insulator 1	4.38E-05	c-14			100.00%		
Winding pack	1.40E-01	nb-94	c-14	ni-63	99.77%	0.00%	0.00%
Insulator 2	1.81E-08	c-14			100.00%		
Outer Coil case	2.38E-07	nb-94	ni-63	tc-99	91.28%	3.50%	1.96%
Cryostat	3.00E-10	nb-94	ni-63	ni-59	98.55%	0.82%	0.44%
Front layer of bioshield	1.42E-11	c-14	nb-94	ni-63	63.29%	35.88%	0.56%
Bioshield1	5.70E-12	c-14	nb-94	ni-63	80.24%	18.61%	0.77%
Bioshield2	1.75E-14	c-14	nb-94	ni-63	90.24%	8.45%	0.89%
Bioshield3	5.28E-18	c-14	nb-94	ni-63	89.59%	8.98%	0.92%
Bioshield4	1.37E-20	c-14	nb-94	ni-63	85.56%	12.87%	0.99%
Between Magnets							
Cryostat	6.51E-07	ni-63	ni-59	c-14	64.51%	35.17%	0.34%
Front layer of bioshield	1.89E-06	c-14	ni-63	ni-59	99.06%	0.77%	0.42%
Bioshield1	9.40E-07	c-14	ni-63	ni-59	98.52%	0.93%	0.51%
Bioshield2	5.24E-09	c-14	ni-63	ni-59	98.54%	0.98%	0.54%
Bioshield3	6.15E-12	c-14	ni-63	ni-59	98.43%	1.12%	0.51%
Bioshield4	5.65E-14	c-14	ni-63	ni-59	98.30%	1.17%	0.50%

Table 12: WDR for NRC-A limits evaluated at 100y after shutdown

Zones	NRCA	Contributor			Contributions%		
W armor	1.05E-01	nb-94	c-14	ni-63	77.75%	11.49%	7.68%
FW1	1.84E+00	nb-94	ni-63	ni-59	78.07%	21.25%	0.70%
BZ1	9.36E-01	nb-94	ni-63	c-14	85.79%	11.75%	1.81%
BW1	1.09E+00	nb-94	ni-63	ni-59	91.86%	7.23%	0.44%
W shell	1.16E-01	c-14	ni-63	tc-99	98.83%	0.64%	0.41%
FW2	8.42E-01	nb-94	ni-63	ni-59	93.30%	6.22%	0.44%
BZ2	2.08E-01	nb-94	ni-63	c-14	92.28%	5.77%	1.34%
BW2	6.97E-02	nb-94	ni-63	ni-59	93.28%	6.43%	0.25%
Structural ring	6.77E-02	nb-94	ni-63	h-3	92.75%	5.83%	1.15%
Vacuum vessel	6.99E-02	nb-94	ni-63	ni-59	92.85%	6.85%	0.22%
Out board shield	1.89E-02	nb-94	ni-63	ni-59	88.72%	10.83%	0.29%
Inner Coil case	3.40E-02	ni-63	nb-94	ni-59	51.15%	44.98%	1.43%
Insulator 1	4.38E-04	c-14	h-3		100.04%	0.00%	
Winding pack	1.40E+00	nb-94	ni-63	c-14	99.76%	0.02%	0.00%
Insulator 2	1.81E-07	c-14	h-3		100.00%	0.00%	
Outer Coil case	3.96E-06	nb-94	ni-63	tc-99	54.85%	41.96%	1.18%
Cryostat	3.47E-09	nb-94	ni-63	ni-59	85.31%	14.15%	0.38%

Front layer of bioshield	1.57E-10	c-14	nb-94	ni-63	57.19%	32.41%	10.13%
Bioshield1	6.53E-11	c-14	nb-94	ni-63	69.96%	16.23%	13.47%
Bioshield2	2.05E-13	c-14	ni-63	nb-94	77.21%	15.20%	7.23%
Bioshield3	6.20E-17	c-14	ni-63	nb-94	76.31%	15.60%	7.65%
Bioshield4	1.63E-19	c-14	ni-63	nb-94	71.96%	16.73%	10.83%
Between Magnets							
cryostat	8.63E-05	ni-63	ni-59	c-14	97.36%	2.65%	0.03%
bioshield1	2.17E-05	c-14	ni-63	ni-59	86.33%	13.53%	0.37%
bioshield2	1.11E-05	c-14	ni-63	ni-59	83.75%	15.83%	0.44%
bioshield3	6.21E-08	c-14	ni-63	ni-59	83.05%	16.58%	0.45%
bioshield4	7.46E-11	c-14	ni-63	ni-59	81.10%	18.50%	0.42%
bioshield5	6.90E-13	c-14	ni-63	ni-59	80.48%	19.14%	0.41%

V.C. Decay Heat

The decay heat is one of the main safety issues during fission reactor accident. Having an excess amount of heat without the ability to cool the components is an important safety issue; hence the decay heat produced in the period of 1 day is of high importance. W generates high decay heat. Since the VV and LT shield 3Cr-3WV FS contains more W than MF82H FS, they produce more decay heat than the SR. The decay heat results can be seen in Figures 25,26,27 and the tungsten contribution can be noted from Tables 13 and 14. It is still the main contributor at 1 day.

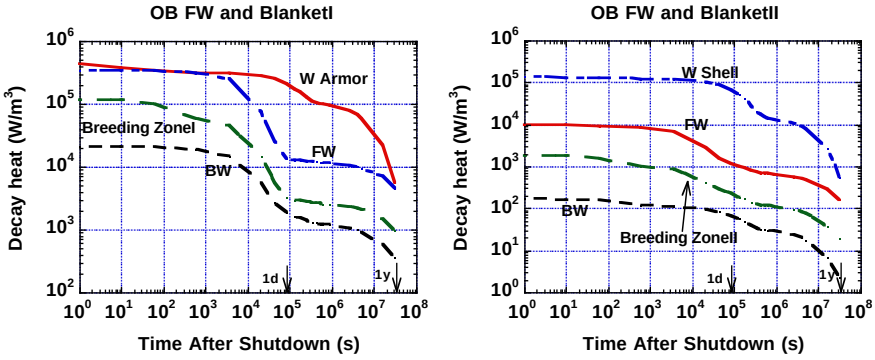

Figure 25: Decay heat of blanket

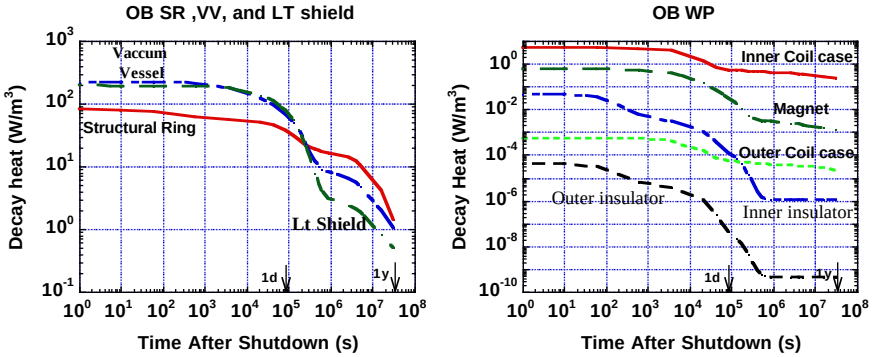

Figure 26: Decay heat of SR, VV, LT shield, and magnet

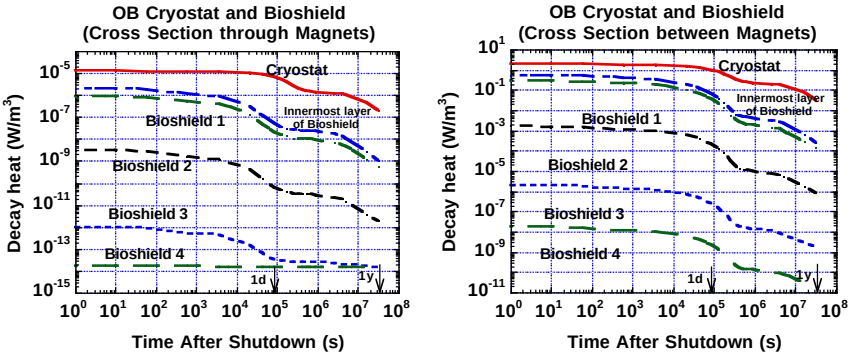

Figure 27: Decay heat of cryostat and bioshield

Table 13: Decay heat contributors at shutdown

Zones	Shutdown	Contributor			Contributions%		
W armor	4.57E+05	w-187	w-183m	w-185	42.05%	21.38%	15.33%
FW1	3.42E+05	mn-56	v-52	mn-54	89.44%	5.23%	2.73%
BZ1	1.18E+05	mn-56	al-28	v-52	46.37%	44.93%	3.03%
BW1	2.10E+04	mn-56	v-52	w-187	78.94%	7.66%	5.23%
W shell	1.36E+05	w-187	w-185	w-183m	78.60%	9.84%	8.15%
FW2	9.70E+03	mn-56	v-52	w-187	72.07%	9.58%	8.74%
BZ2	1.84E+03	al-28	mn-56	w-187	33.32%	32.28%	11.00%
BW2	1.67E+02	w-187	v-52	mn-56	43.18%	26.31%	6.94%
Structural ring	8.48E+01	w-187	v-52	ta-182	43.50%	22.52%	8.25%
Vacuum vessel	2.23E+02	w-187	mn-56	v-52	51.98%	36.84%	4.17%
Out board shield	1.98E+02	w-187	mn-56	w-183m	75.12%	17.85%	3.52%
Inner Coil case	4.84E+00	mn-56	co-60	mo-99	83.89%	5.25%	2.58%
Insulator 1	4.54E-02	al-28	si-31	na-24	90.65%	7.97%	0.80%
Winding pack	5.73E-01	mn-56	cu-64	cu-66	66.37%	16.09%	11.89%
Insulator 2	4.12E-05	al-28	si-31	na-24	87.60%	11.82%	0.26%
Outer Coil case	5.45E-04	mn-56	co-60	mo-99	84.02%	4.48%	3.05%
Cryostat	1.31E-05	w-187	ta-182	w-183m	80.01%	7.70%	4.48%
Front layer of bioshield	1.98E-06	mn-56	al-28	si-31	49.69%	39.53%	4.66%
Bioshield1	9.43E-07	mn-56	al-28	k-42	48.55%	44.31%	3.39%
Bioshield2	3.14E-09	mn-56	al-28	k-42	47.47%	46.51%	3.22%
Bioshield3	9.68E-13	al-28	mn-56	k-42	46.47%	45.95%	3.10%
Bioshield4	1.74E-14	mo-98	al-28	mn-56	81.57%	6.84%	6.26%
Between Magnets							
Cryostat	2.01E+00	w-187	ta-182	w-183m	78.12%	8.01%	4.47%
Front layer of bioshield	5.51E-01	na-24	mn-56	al-28	32.30%	31.76%	26.31%
Bioshield1	2.98E-01	na-24	mn-56	al-28	34.25%	30.32%	27.94%
Bioshield2	1.67E-03	na-24	mn-56	al-28	35.00%	29.32%	28.96%
Bioshield3	2.00E-06	na-24	al-28	mn-56	33.14%	31.34%	28.63%
Bioshield4	1.82E-08	na-24	al-28	mn-56	32.81%	31.55%	28.64%

Table 14: Decay heat contributors at 1 day

Zones	1 day	Contributor			Contributions%		
W armor	2.05E+05	w-187	w-185	w-181	46.64%	33.82%	7.65%
FW1	1.35E+04	mn-54	cr-51	w-187	69.17%	6.39%	5.86%
BZ1	3.25E+03	mn-54	w-187	w-185	60.08%	13.71%	4.78%
BW1	1.85E+03	mn-54	w-187	fe-59	37.75%	29.58%	8.44%
W shell	6.86E+04	w-187	w-185	re-186	77.72%	19.39%	1.08%
FW2	1.14E+03	w-187	mn-54	fe-59	36.95%	26.44%	10.68%
BZ2	2.23E+02	w-187	fe-59	mn-54	44.91%	13.61%	12.89%
BW2	6.74E+01	w-187	ta-182	fe-59	53.44%	16.33%	13.49%
Structural ring	3.67E+01	w-187	ta-182	w-185	50.13%	18.94%	14.22%
Vacuum vessel	6.66E+01	w-187	w-185	fe-59	86.34%	6.85%	4.49%
Out board shield	7.77E+01	w-187	w-185	fe-59	95.49%	1.92%	1.48%
Inner Coil case	5.47E-01	co-60	ta-182	mo-99	46.47%	22.68%	17.80%
Insulator 1	1.27E-04	na-24	si-31	c-14	94.00%	4.99%	0.82%
Winding pack	2.98E-02	cu-64	sb-125	in-113m	83.45%	3.20%	2.54%
Insulator 2	4.43E-08	na-24	si-31	c-14	79.85%	19.20%	0.97%
Outer Coil case	5.57E-05	co-60	mo-99	ta-182	43.84%	23.18%	18.33%
Cryostat	6.73E-06	w-187	ta-182	fe-59	77.40%	15.00%	3.08%
Front layer of bioshield	5.09E-08	fe-59	k-42	cu-64	48.55%	40.49%	4.60%
Bioshield1	2.09E-08	fe-59	k-42	cu-64	48.28%	**39.82%**	4.70%
Bioshield2	6.51E-11	fe-59	k-42	cu-64	46.87%	40.26%	4.73%
Bioshield3	3.52E-14	mo-98	fe-59	k-42	40.31%	25.83%	22.20%
Bioshield4	1.50E-14	mo-98	ca-48	fe-59	94.58%	4.82%	0.15%
Between Magnets							
Cryostat	1.03E+00	w-187	ta-182	fe-59	75.97%	15.56%	3.45%
Front layer of bioshield	6.78E-02	na-24	fe-59	k-42	86.40%	6.44%	5.40%
Bioshield1	3.77E-02	na-24	fe-59	k-42	88.75%	5.27%	4.37%
Bioshield2	2.14E-04	na-24	fe-59	k-42	89.56%	4.71%	4.01%
Bioshield3	2.46E-07	na-24	fe-59	k-42	88.78%	4.76%	4.05%
Bioshield4	2.22E-09	na-24	fe-59	k-42	88.19%	4.86%	4.10%

V.D. Recycling

As shown by the WDR analysis, fusion produces only LLW, which offers an advantage over fission, but it also produces large quantities of LLW that suggests the need to develop a new strategy other than the geologic disposal. Recycling and Clearing are two strategies that are endorsed by fusion. Recycling is the reuse of material by the nuclear industry, while clearance is the unconditional release of slightly radioactive materials to the commercial market to be fabricated as consumer products. As the limited capacity of storing LLW along with the political difficulty of building new HLW and LLW repositories increases, the difficulty in dealing with the disposal of large quantities of fusion LLW increases. Hence, the new strategies have the advantage of reclaiming resources by recycling, which leads to the minimization of the rad-waste burden for

future generations and promote fusion as nuclear energy source with minimal environmental impact [7]. This is the rationale for performing recycling and clearance analyses on all fusion components and their individual constituents.

Figures 28,29,30 show that all materials are recyclable with advance remote handling (RH) equipment at a short time after shutdown (within 1 day), even for the FW, which is subjected to the highest neutron flux.

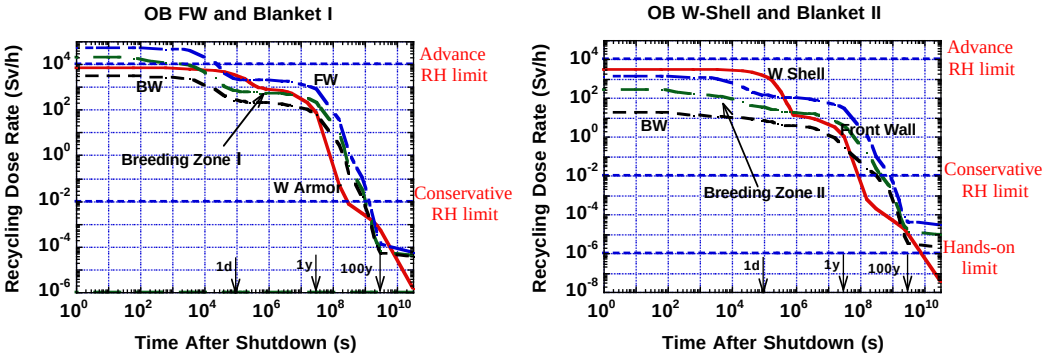

Figure 28: Recycling for Blanket Regions

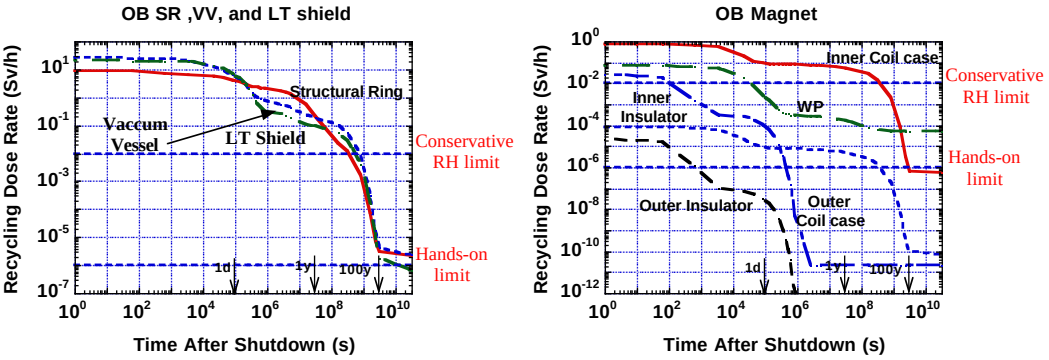

Figure 29: Recycling for SR, VV, LT shield, and magnet

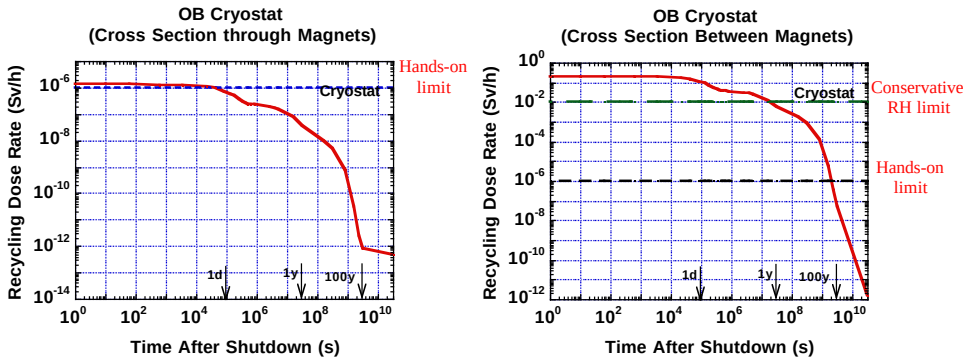

Figure 30: Recycling for Cryostat Region

Recycling and clearance should be done for constituents rather than for the entire component [8]. Hence we examined the individual constituents in Figures 31-37.

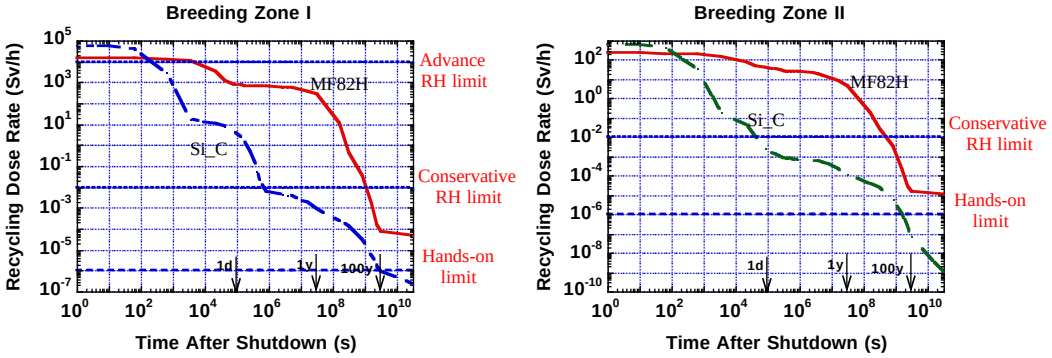

Figure 31: Recycling of constituents of breeding zones.

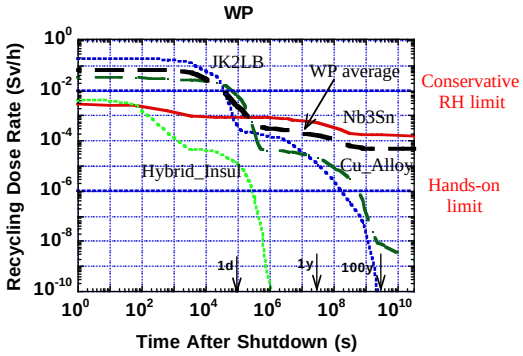

Figure 32: Recycling of constituents for WP

Regarding the difference of paths taken before reaching the bioshield, the higher neutron flux doesn't exclude the constituents from being recyclable, but rather requires different recycling technology. The graphs for regions affect by difference in paths, are plotted next to each other in Figures 33-37 for comparison. It is to be noted that, for many components, the main contributor to the recycling dose at one year after shutdown is Mn-54 as see in Table 15.

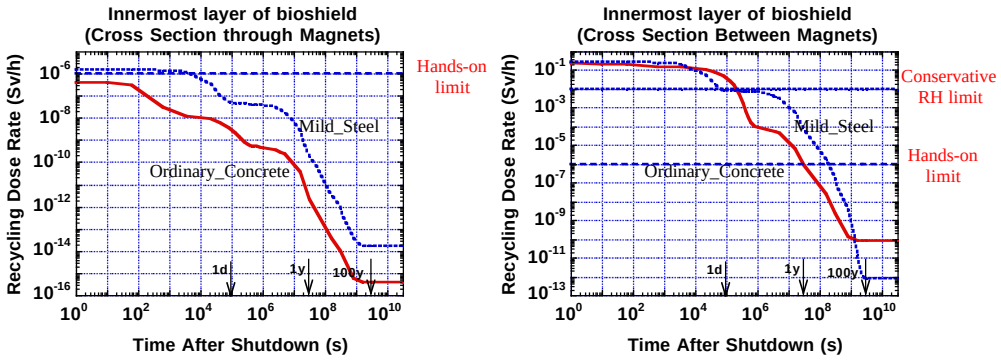

Figure 33: Recycling per path for innermost layer of bioshield

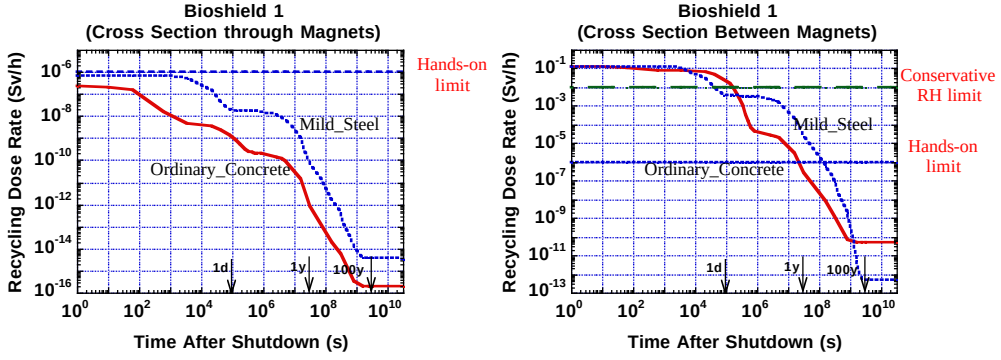

Figure 34: Recycling per path for first layer of bioshield

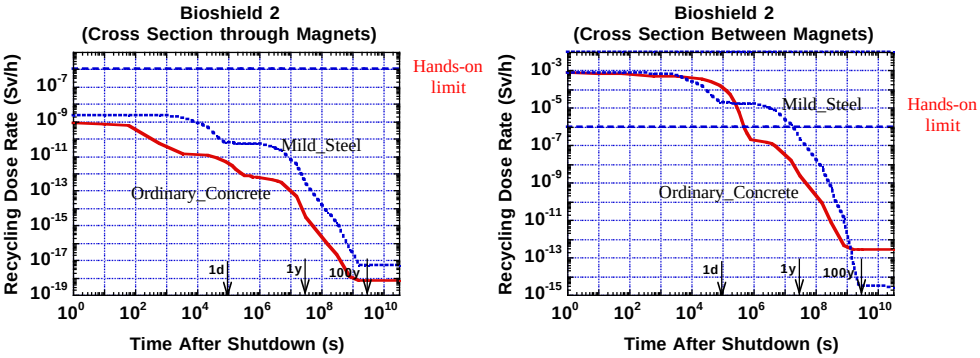

Figure 35: Recycling per path for second layer of bioshield

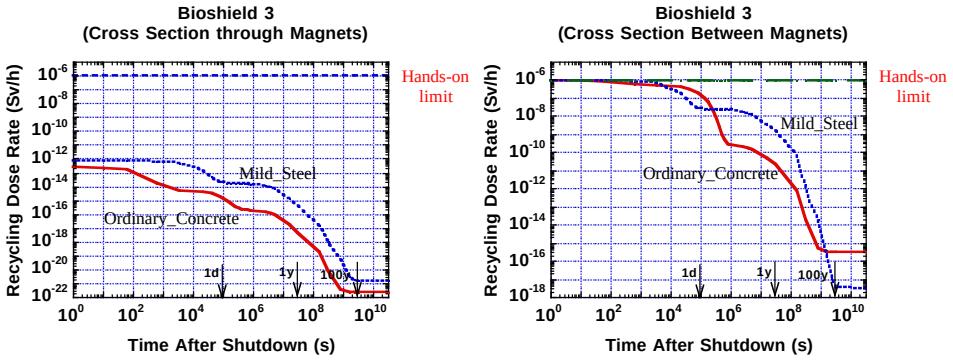

Figure 36: Recycling per path for third layer of bioshield

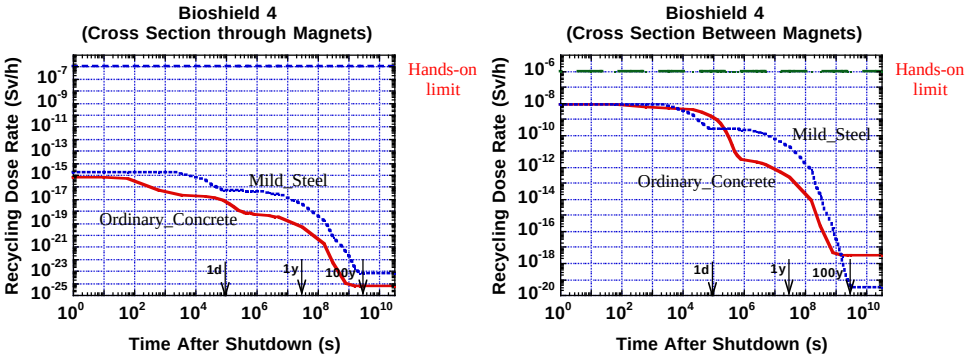

Figure 37: Recycling per path for fourth layer of bioshield

Table 15: Recycling contributors at 1 year after shutdown

Zones	1 year	Contributor			Contributions%		
W armor	6.77E+01	ta-182	re-184	re-184m	82.00%	12.78%	3.74%
FW1	8.29E+02	mn-54	ta-182	co-60	98.96%	0.59%	0.30%
BZ1	2.17E+02	mn-54	ta-182	co-60	98.08%	1.38%	0.33%
BW1	6.49E+01	mn-54	ta-182	co-60	94.60%	4.47%	0.58%
W shell	1.10E+00	ta-182	re-184	w-181	92.08%	4.29%	2.22%
FW2	2.92E+01	mn-54	ta-182	co-60	91.20%	7.68%	0.84%
BZ2	3.93E+00	mn-54	ta-182	co-60	79.93%	17.56%	1.62%
BW2	3.16E-01	ta-182	mn-54	co-60	67.48%	18.98%	11.41%
Structural ring	1.99E-01	ta-182	co-60	mn-54	67.89%	19.11%	11.26%
Vacuum vessel	1.79E-01	co-60	mn-54	fe-59	96.67%	1.65%	1.17%
Out board shield	9.38E-02	co-60	fe-59	mn-54	98.01%	0.86%	0.73%

Inner Coil case	5.05E-02	co-60	ta-182	mn-54	95.06%	4.75%	0.13%
Insulator 1	2.10E-11	al-26			100.00%		
Winding pack	1.62E-04	sb-125	nb-94	in-113m	57.23%	31.82%	4.63%
Insulator 2	4.32E-15	al-26			100.00%		
Outer Coil case	4.81E-06	co-60	ta-182	fe-59	95.82%	4.09%	0.03%
Cryostat	3.67E-08	ta-182	co-60	fe-59	53.09%	46.29%	0.39%
Front layer of bioshield	4.99E-11	fe-59	mn-54	fe-55	91.25%	4.39%	4.31%
Bioshield1	2.02E-11	fe-59	fe-55	mn-54	91.58%	5.74%	2.52%
Bioshield2	6.75E-14	fe-59	mn-54	fe-55	83.26%	10.70%	6.04%
Bioshield3	1.04E-16	mn-54	fe-59	fe-55	82.42%	16.12%	1.17%
Bioshield4	1.00E-18	mn-54	fe-59	fe-55	95.33%	4.14%	0.28%
Between Magnets							
Cryostat	6.18E-03	ta-182	co-60	mn-54	49.97%	48.35%	1.05%
Front layer of bioshield	1.87E-05	mn-54	fe-59	fe-55	55.09%	42.95%	2.09%
Bioshield1	6.33E-06	fe-59	mn-54	fe-55	57.81%	38.54%	3.63%
Bioshield2	5.60E-08	mn-54	fe-59	fe-55	64.51%	33.06%	2.38%
Bioshield3	4.59E-10	mn-54	fe-59	fe-55	94.89%	4.68%	0.33%
Bioshield4	5.16E-12	mn-54	fe-59	fe-55	95.87%	3.85%	0.26%

V.E. Clearance

Although all components are considered recyclable with RH equipment, our analysis has shown that only the outer regions of the magnet, cryostat and bioshield are clearable (CI<1) specifically for regions shielded by the magnets as shown in Figures 38,39,40. For the regions not protected by the magnets an extra 8 cm of LT shield would be required to make all the bioshield components clearable within 100 years. Figure 41 shows why performing the clearance by constituents is of great importance. The WP as a whole may not be clearable, but 25% of its composition (Cu) can be cleared within 100 years. Figures 42-46 compare the clearance index of both pathways and Table 16 shows the main contributors for regions classified as clearable for a pathway through magnets. As pointed out earlier and shown in figure 40, the innermost layer of bioshield between magnets is not clearable unless the LT shield is augmented by 8 cm.

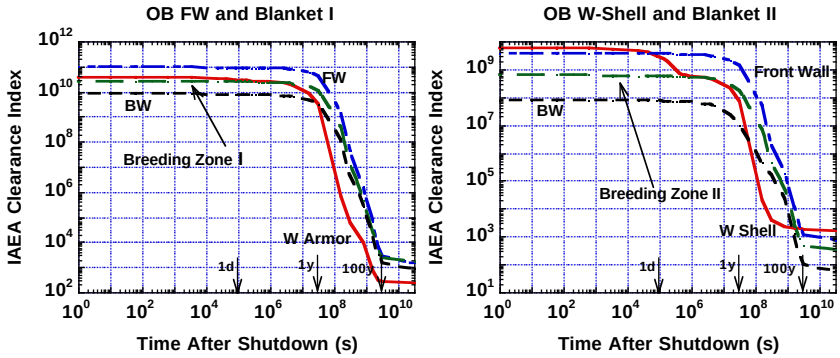

Figure 38: Clearance for Blanket regions

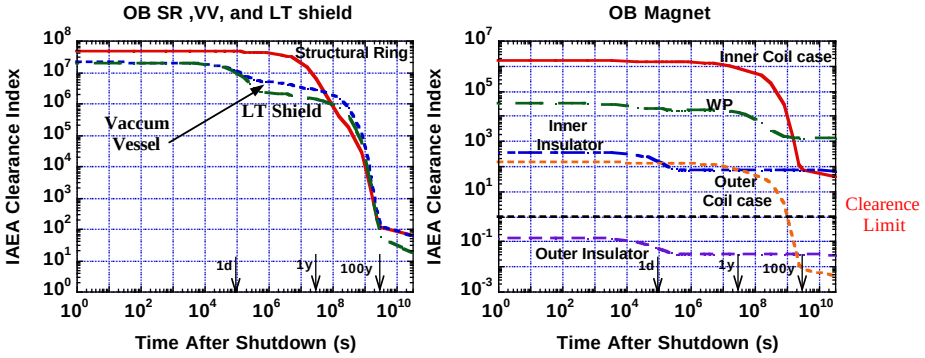

Figure 39: Clearance for SR, VV, LT shield, and magnet

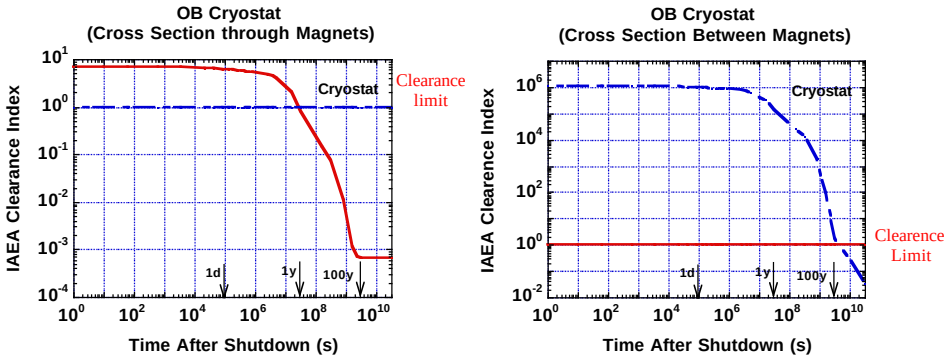

Figure 40: Clearance for Cryostat region

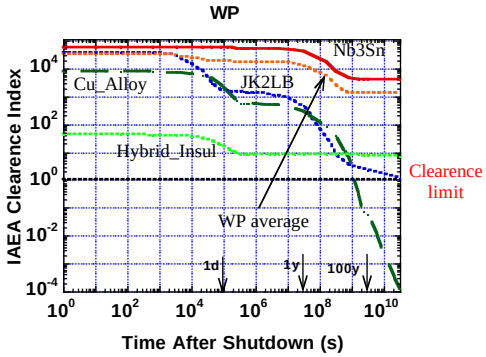

Figure 41: Clearance index for WP

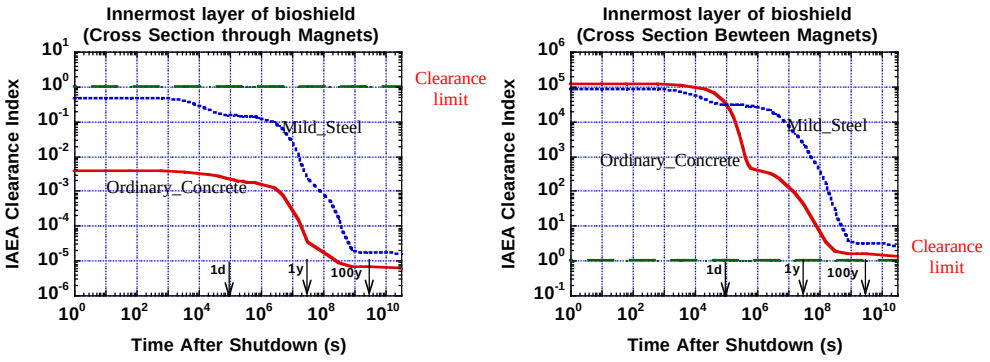

Figure 42: Clearance index for innermost layer of bioshield

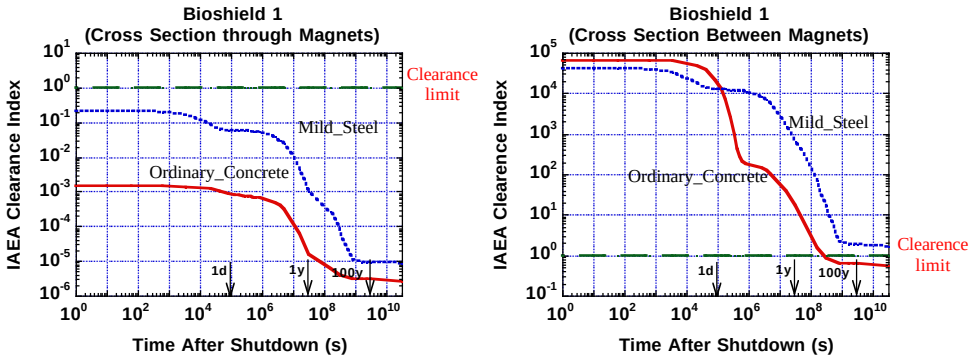

Figure 43: Clearance index for first layer of bioshield

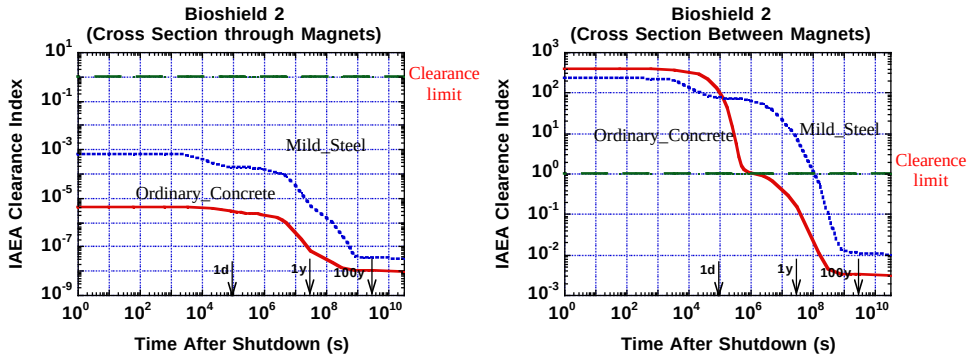

Figure 44: Clearance index for second layer of bioshield

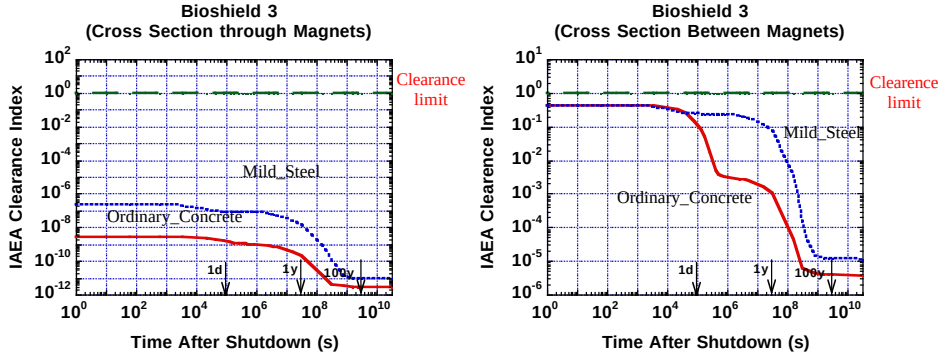

Figure 45: Clearance index for Third layer of Bioshield

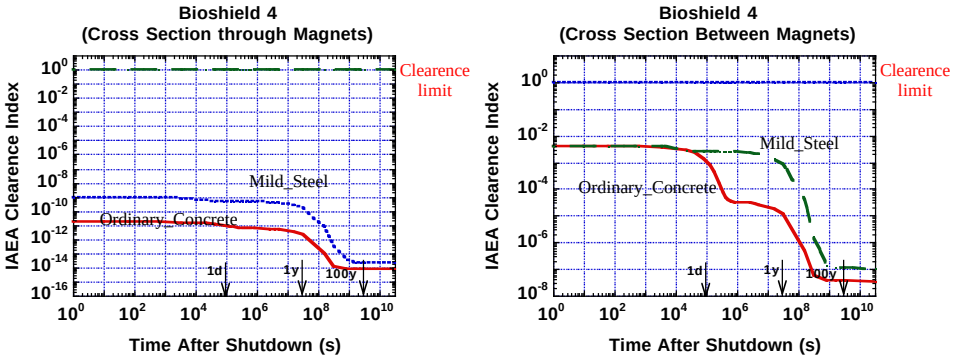

Figure 46: Clearance index for Forth layer of Bioshield

Table 16: Clearance index contributors at shutdown

Clearance Index of whole regions for cross section through magnet								
Zones	Time	Value	Contributor			Contributions %		
Insulator 2	Shutdown	1.38E-01	na-24	c-14	si-31	57.73%	21.76%	20.51%
Outer Coil case	5 years	1.14E-01	co-60	ni-63	nb-94	92.52%	3.36%	1.78%
Cryostat	1 year	8.37E-01	ta-182	co-60	eu-152	70.95%	28.47%	0.16%
Front layer of bioshield	Shutdown	1.28E-01	mn-56	fe-59	k-42	65.45%	32.45%	0.79%
Bioshield1	Shutdown	5.72E-02	mn-56	fe-59	k-42	68.55%	29.73%	0.72%
Bioshield2	Shutdown	1.83E-04	mn-56	fe-59	k-42	69.88%	28.06%	0.70%
Bioshield3	Shutdown	6.46E-08	mn-56	fe-59	mn-54	58.99%	23.69%	14.79%
Bioshield4	Shutdown	2.47E-10	mn-54	mn-56	fe-59	43.35%	37.80%	15.44%

Observations: Nb-94 is the main WDR contributor to zones that contain MF82H. Using isotope tracing, we find that the main source of Nb-94 is Nb through (n,γ) reactions; hence the removal of Nb from the original mixture gives WDR seen in Table 17 where all values are below 0.1, qualifying all materials as Class A LLW. Nb-94 is also the main contributor for the vacuum vessel. Due to the presence of Nb-94 and W-187 the vacuum vessel is not a clearable component, but a vacuum vessel made completely out of pure Fe can be cleared in less than 100 years as seen in Figure 47. Controlling the Nb impurity and W alloying elements allows the VV to be cleared for commercial market use.

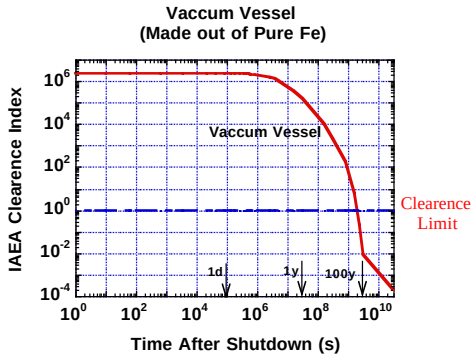

Figure 47: Vacuum vessel made of Pure Fe

Table 17: Fetter Lo WDR after isotopic tailoring

Fetter Lo at 100 years		
Remove Isotopes that produce	Zone	WDR
nb-93	FW1	0.09
nb-93	BZ1	0.03
nb-93	BW1	0.03
nb-93	W/FW/Blanket	0.04

Since the FW/blanket and W-armor produce more decay heat than any other component, isotopic tailoring can be used for the removal of sources of Mn-54 and W-187, which are the main contributors at 1 Day. This helps reduce the decay heat and the new decay heat produced is displayed in Table 18 for the FW/blanket.

Table 18: Decay heat at 1 day after isotopic tailoring

Decay heat		
Remove Isotopes that produce Mn-54	Zone	1 Day
fe-54	FW1	4346.97
fe-54	BZ1	1308.92
fe-54	BW1	1151.70

VI.Conclusions

Shielding analysis results show that the optimum composition is 45% B-FS filler, 50% H2O and 5% FS ribs for the LT shield middle regions. This composition satisfies all the magnet radiation limits. A large percentage of the total nuclear heating takes place in the breeding zones where have high dpa, He and H production. Those parameters decrease as we move out radially. The He and H productions decrease faster than the dpa. Also, as we move out radially, the neutron spectrum gets softer, unlike the gamma spectrum that just decreases in magnitude.

All components are Class A LLW except FW/blanket; controlling the Nb impurity qualifies the FW/blanket as Class A LLW. Isotopic tailoring decreases the decay heat. All components are not recyclable shortly after shutdown. Only the cryostat and bioshield components behind the magnets are clearable. In the regions between magnets, ~8 cm of additional LT shield is needed to clear the cryostat and bioshield before 100 years. Vacuum vessel can also be made clearable if the W alloying element and Nb impurity are controlled.

VII.Acknowledgments

Professor Mohammed Sawan, Professor Doug Henderson, Professor Paul Wilson, and Dr. Andy Davis (UW), Dr. Walid Metwally (UoS) provided great support for this work. The FESS-FNSF nuclear-related work at UW-Madison is supported by the US Department of Energy.

VIII.References

1. L. El-Guebaly, S. Malang, A. Rowcliffe, and L. Waganer, "Blanket/Materials Testing Strategy for FNSF and its Breeding Potential," Fusion Sci. Technol., Vol. 68 (2015); http://dx.doi.org/10.13182/FST15-124.
2. B. Madani and L. El-Guebaly, "Shielding and Activation Analyses for Inboard Region of FESS-FNSF Design," University of Wisconsin Fusion Technology Institute Report, UWFDM-1423 (November 2015). Available at: http://fti.neep.wisc.edu/pdf/fdm1423.pdf.
3. L. El-Guebaly and L. Mynsberge, "Neutronics Characteristics, Shielding System, Activation and Environmental Aspects of ARIES-ACT-2 Power Plant," University of Wisconsin Fusion Technology Institute Report, UWFDM-1418 (2014). Available at: http://fti.neep.wisc.edu/pdf/fdm1418.pdf.
4. El-Guebaly, L., & Desecures, M. (2012). *Environmental Aspects of W-Based Components Employed in ITER, ARIES, and PPCS Fusion Designs.* University of Wisconsin Fusion Technology Institute. Madison: University of Wisconsin Fusion Technology Institute.
5. US Code of Federal Regulations, Title 10, Energy, Part 61, Licensing Requirements for Land Disposal of Radioactive Waste, Section 55, Waste classification, US Government Printing Office, January 2014.
6. S. FETTER, E.T. CHENG, and F.M. MANN, "Long Term Radioactive Waste from Fusion Reactors: Part II," Fusion Engineering and Design, **13**, 239-246 (1990).
7. L. A. EL-GUEBALY, "Future Trend Toward the Ultimate Goal of Radwaste-Free Fusion: Feasibility of Recycling/Clearance, Avoiding Geological Disposal." Journal of Plasma and Fusion Research, **8**, 3404041-1-6 (2013).
8. L. EL-GUEBALY, "Evaluation of Disposal, Recycling, and Clearance Scenarios for Managing ARIES Radwaste after Plant Decommissioning," Nuclear Fusion, 47, 485 (2007).
9. D. Henderson, L. El-Guebaly, P. Wilson, and A. Abdou, "Activation, Decay Heat, and Waste Disposal Analysis for ARIES-AT Power Plant," Fusion Technology, **39**, No. 2, 444 (2001).
10. DANTSYS: A Diffusion Accelerated Neutral Particle Transport Code System, Los Alamos National Laboratory Report, LA-12969-M (1995).
11. D. L. ALDAMA and A. TRKOV, "FENDL-2.1 Update of an Evaluated Nuclear Data Library for Fusion Applications," International Atomic Agency Report INDC(NDC)-467 (2004).
12. P. WILSON and D. HENDERSON, "ALARA: Analytic and Laplacian Adaptive Radioactivity Analysis: A Complete Package for Analysis of Induced Activation," University of Wisconsin Fusion Technology Institute Report. Volume I - UWFDM-1070. Volume II - UWFDM-1071 (1998). ALARA user's guide: https://trac.cae.wisc.edu/trac/svalinn/wiki/ALARAInputFileSyntax.
13. FENDL3 Activation Library: https://www-nds.iaea.org/fendl3/000pages/StarterLib/2011-12-01/.